AWARD NUMBER: W81XWH-17-1-0268

TITLE: Investigating the Role of Creatine in Oligodendrocyte Regeneration During CNS Remyelination

PRINCIPAL INVESTIGATOR: Jeffrey K. Huang

CONTRACTING ORGANIZATION: Georgetown University

REPORT DATE: OCTOBER 2021

TYPE OF REPORT: FINAL REPORT

PREPARED FOR: U.S. Army Medical Research and Development Command
Fort Detrick, Maryland 21702-5012

REPORT DOCUMENTATION PAGE

Form Approved
OMB No. 0704-0188

1. REPORT DATE	**2. REPORT TYPE**	**3. DATES COVERED**
OCTOBER 2021	Final	15Jun2017-14Jun2021

4. TITLE AND SUBTITLE

Investigating the Role of Creatine in Oligodendrocyte Regeneration During CNS Remyelination

5a. CONTRACT NUMBER
W81XWH-17-1-0268

5b. GRANT NUMBER

5c. PROGRAM ELEMENT NUMBER

6. AUTHOR(S)

Jeffrey K. Huang

E-Mail: jh1659@georgetown.edu

5d. PROJECT NUMBER

5e. TASK NUMBER

5f. WORK UNIT NUMBER

7. PERFORMING ORGANIZATION NAME(S) AND ADDRESS(ES)

Georgetown University
Washington DC 20057

8. PERFORMING ORGANIZATION REPORT NUMBER

9. SPONSORING / MONITORING AGENCY NAME(S) AND ADDRESS(ES)

U.S. Army Medical Research and Development Command
Fort Detrick, Maryland 21702-5012

10. SPONSOR/MONITOR'S ACRONYM(S)

11. SPONSOR/MONITOR'S REPORT NUMBER(S)

12. DISTRIBUTION / AVAILABILITY STATEMENT

Approved for Public Release; Distribution Unlimited

13. SUPPLEMENTARY NOTES

14. ABSTRACT:

The goal of this study is to test the hypothesis that rOL protection through creatine improves CNS remyelination. To this end, we will determine i) if creatine synthesis in rOLs is required for rOL survival and remyelination, ii) if diminished creatine levels and rOL integrity contribute to remyelination impairment associated with aging, and iii) if the systemic administration of creatine and cyclocreatine (a blood brain barrier permeable creatine analog) can improve CNS remyelination. We will also determine iv) what transcripts and pathways in rOLs are affected with creatine deficiency.

15. SUBJECT TERMS

None Listed

16. SECURITY CLASSIFICATION OF:			**17. LIMITATION OF ABSTRACT**	**18. NUMBER OF PAGES**	**19a. NAME OF RESPONSIBLE PERSON**
a. REPORT	**b. ABSTRACT**	**c. THIS PAGE**			USAMRDC
Unclassified	Unclassified	Unclassified	Unclassified	48	**19b. TELEPHONE NUMBER** *(include area code)*

TABLE OF CONTENTS

1. **INTRODUCTION:** *Narrative that briefly (one paragraph) describes the subject, purpose and scope of the research.*
The goal of this study is to test the hypothesis that rOL protection through creatine improves CNS remyelination. To this end, we will determine i) if creatine synthesis in rOLs is required for rOL survival and remyelination, ii) if diminished creatine levels and rOL integrity contribute to remyelination impairment associated with aging, and iii) if the systemic administration of creatine and cyclocreatine (a blood brain barrier permeable creatine analog) can improve CNS remyelination. We will also determine iv) what transcripts and pathways in rOLs are affected with creatine deficiency.

2. **KEYWORDS:** *Provide a brief list of keywords (limit to 20 words).*
Creatine, guanidinoacetate methyltransferase (GAMT), remyelination, oligodendrocytes, transgenic mice, experimental demyelination, aging.

3. **ACCOMPLISHMENTS:** *The PI is reminded that the recipient organization is required to obtain prior written approval from the awarding agency grants official whenever there are significant changes in the project or its direction.*

What were the major goals of the project?
Aim 1, Major Task 1: Analyze rOL viability and remyelination in OL-specific Gamt knockout mouse.
Subtasks: Perform lysolecithin-mediated demyelination on conditional Gamt knockout mice; perfuse mice; perform immunostaining analysis; perform electron microscopy.
Percentage of Task Completion: 90% ; We were unable to obtain enough tissues for electron microscopy.

Aim 1, Major Task 2: Analyze effect of creatine/cyclocreatine administration on rOL survival and remyelination in Gamt deficient mice.
Subtasks: Perform lysolecithin-mediated demyelination on Gamt KO and WT mice; Feed with creatine, cyclocreatine, or regular diet; perfuse and section; perform immunostaining analysis; perform electron microscopy.
Percentage of Task Completion: 100%

Aim 2, Major Task 1: Compare creatine levels and rOL survival between aged and young mice.
Subtasks: Perform lysolecithin-mediated demyelination on young and old mice; perform immunostaining analysis; perform PCR/western blot; perform electron microscopy.
Percentage of Task Completion: 90% ; We were unable to obtain enough tissues for electron microscopy.

Aim 2, Major Task 2: Analyze effect of systemic creatine/cyclocreatine administration on rOL survival and remyelination in aged mice.
Subtasks: Perform lysolecithin-mediated demyelination on aged mice; Feed with creatine, cyclocreatine, or regular diet; perfuse and section; perform immunostaining analysis; perform electron microscopy.
Percentage of Task Completion: 100%

Aim 3, Major Task: Perform genomic analysis of CNS tissues from GAMT KO and WT mice.

Subtasks: Dissected CNS tissues (brain); purified single nuclei, generated library and perform single nuclei analysis; validate gene expression by PCR or in situ hybridization.
Percentage of Task Completion: 75%. Single nuclei RNAseq was performed, but additional RNAseq study needs to be performed for validation studies.

What was accomplished under these goals?

1. Endogenously synthesized creatine supplies cerebral creatine and is dependent on Gamt expression. To determine if cerebral creatine is detectable in the absence of Gamt expression, we performed 1H-magnetic resonance spectroscopy (MRS) analysis in the prefrontal cortex of eight-week old Gamt knockout (KO) (Fig. 1a) and wild-type (WT) mice (Fig. 1b). We found that the KO mice on a standard rodent diet displayed measurable, but significantly lower creatine levels in the brain compared to WT (Fig. 1d), suggesting that dietary creatine can partially compensate for cerebral creatine levels when GAMT is missing. MRS analysis was also performed on KO and WT mice on a creatine deficient diet. We found that WT mice on creatine deficient diet displayed similar creatine levels as those on standard diet. By contrast, Gamt KO mice on creatine deficient diet displayed undetectable creatine levels in the prefrontal cortex (Fig. 1d). These data suggest that endogenously synthesized creatine can supply adequate cerebral creatine in the absence of dietary creatine, and that GAMT is the main enzyme responsible for creatine synthesis in the mouse brain. Moreover, our data also suggest that dietary creatine can supply cerebral creatine in the absence of Gamt expression in mice, providing an explanation for the lack of obvious myelination impairment in our previous study (Chamberlain et al., 2017). To examine the effect of Gamt deletion on postnatal CNS development, all subsequent studies were performed on mice on creatine deficient diet.

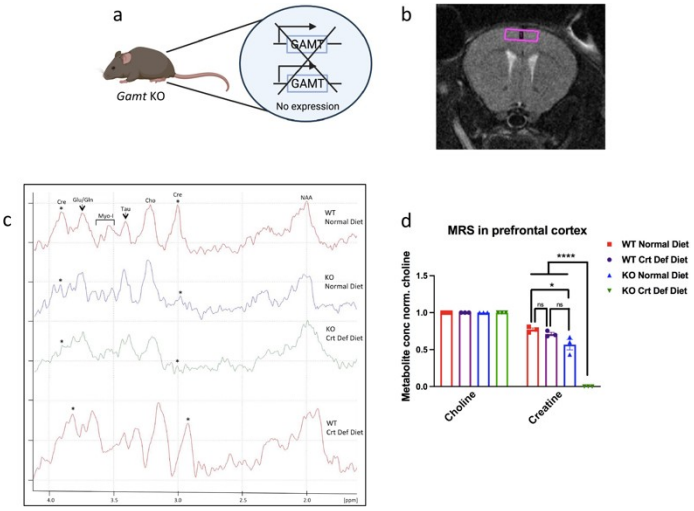

Fig 1. Endogenously synthesized creatine supplies cerebral creatine and is dependent on Gamt expression. a) Diagram of Gamt knockout (KO) transgenic mouse model b) Region of magnetic resonance spectroscopy (MRS) voxel placement in mouse prefrontal cortex c) Representative trace from MRS from each group d) Quantification of metabolites, normalized to choline, showing unmeasurable creatine levels in the brain in the KO on creatine deficient diet (one-way ANOVA with Tukey's multiple comparisons; F (3, 8)=83.81, df=11, $p<0.0001$) and normal levels of creatine in the WT on creatine deficient diet (WT normal vs. WT crt def $p=0.70$, ns). KO on a normal diet had measurable, but significantly reduced levels of creatine compared to WT (KO normal vs. WT normal $p=0.02$). All data presented as mean±SEM with n=3 biological replicates. Data presented with *$p<0.05$, **$p<0.01$, ***$p<0.001$, ****$p<0.0001$, ns= not significant.

2. Gamt knock-in reporter mouse line reveals mature oligodendrocytes are the major producers of creatine in the postnatal CNS. We developed a transgenic mouse model that expresses a green fluorescent protein (GFP) reporter upon the conditional excision of Gamt. This mouse line (Gamtfl/fl) contains LoxP sites flanking exons 2-6 of the Gamt gene (Fig. 2a). To delete Gamt developmentally and in all tissues, Gamtfl/fl were crossed with a cytomegalovirus Cre recombinase-expressing mouse line (CMV-Cre). Heterozygous mice containing one copy of Gamt (GamtGFP/+) were used to track

CNS cell populations that synthesize creatine while the mice with homozygous deletion (GamtGFP/GFP) were used for Gamt loss-of-function analysis. Controls are Gamtfl/fl without Cre recombinase. Immunohistochemistry was performed to co-localize GFP expression within CNS cell types in the cortex from postnatal (P) day P0 until P60.

We observed low, but widespread GFP expression in neuroblasts/neural stem cells (Fig. 2b), neurons (Fig. 2c), oligodendrocytes (Fig. 2d), and astrocytes (Fig. 2e) at P0 and P7, which supports previously published Gamt expression data (Tachikawa et al., 2018). However, by P14, when large-scale active developmental myelination is occurring (Sturrock, 1980), this wide-spread expression was no longer observed, and GFP expression appeared to be restricted to distinctive cell populations in the CNS. We found that GFP was not expressed in GFAP+ astrocytes (Fig. 2f), Iba1+ microglia (Fig. 2g), or NeuN+ neurons (Fig. 2h), but was strongly expressed in Olig2+ oligodendrocyte lineage cells in corpus callosum (Fig. 2i). To further determine when endogenous creatine synthesis occurs during oligodendrocyte lineage cell progression, immunostaining analysis for GFP expression and NKX2.2+ OPCs, BCAS1+ premyelinating oligodendrocytes, and CC1+ mature oligodendrocytes was performed. We found that GFP was undetectable in OPCs (Fig. 2j), expressed in few premyelinating oligodendrocytes (Fig. 2k), and abundantly expressed in mature oligodendrocytes (Fig. 2l). Quantification revealed GFP expression in approximately 17% of premyelinating oligodendrocytes and 95% of mature oligodendrocytes (Fig. 2m). These results suggest that during active myelination, endogenous creatine synthesis in the adult CNS occurs exclusively in oligodendrocytes during their maturation.

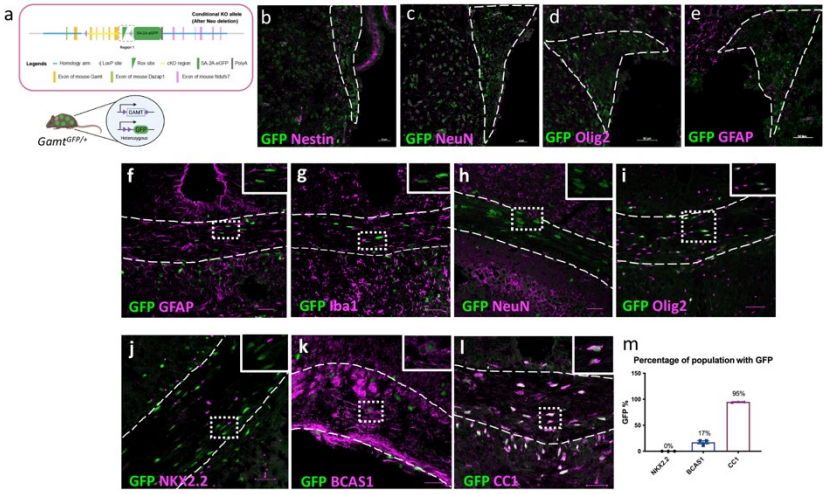

Fig 2. Gamt knock-in reporter mouse shows Gamt becomes highly expressed and restricted to oligodendrocyte lineage cells during active myelination. a) Diagram of transgenic mouse model showing heterozygous expression of Gamt with GFP expression. Postnatal (P) day P7 co-immunostaining analysis of GFP and b) Nestin+ cells around the subventricular zone (SVZ), c) Nestin+ cells at the adjacent striatum, d) Olig2+ oligodendrocyte lineage cells, and e) GFAP+ astrocytes in the corpus callosum. SVZ is outlined in white dotted line b-e. P14 co-immunostaining analysis of GFP and f) GFAP+ astrocytes, g) Iba1+ microglia/macrophages, h) NeuN+ neurons, i) Olig2+ oligodendrocyte lineage cells, j) NKX2.2+ OPCs, k) BCAS1+ premyelinating oligodendrocytes, and l) CC1+ oligodendrocytes in the corpus callosum. m) Percentage of OPCs, premyelinating and mature oligodendrocytes that express GFP. All data presented as mean±SEM with n=3 biological replicates. Scale bar is 20µm in b,c and 50µm in all other images.

3. Gamt deletion leads to reduced mature oligodendrocyte survival and delayed myelination.

We next determined the impact of Gamt loss-of-function on CNS myelination in homozygous GamtGFP/GFP, and control Gamtfl/fl (WT) mice. To confirm Gamt deletion, western blot analysis for GAMT protein expression in brain extracts of WT and GamtGFP/GFP mice at P21 were performed. We observed a complete loss of GAMT expression (26 kDa) in GamtGFP/GFP mice compared to control, indicating Gamt was effectively deleted in the CNS of GamtGFP/GFP mice (Fig. 3a). Next, we compared the total number of oligodendrocyte lineage cells in the corpus callosum in GamtGFP/GFP and control mice by immunostaining analysis (Fig. 3b). We observed a significant reduction of total Olig2+ oligodendrocyte lineage cell numbers at P14 and a trending decrease at P21 in GamtGFP/GFP mice compared to control (Fig. 3c; top). Moreover, we observed a significant decrease of CC1+ mature oligodendrocytes in GamtGFP/GFP mice at P14 and P21 (Fig 3c; bottom). However, this reduction in total number of oligodendrocytes was no longer significant by P60 (Fig 3c). We also examined the number of NKX2.2 OPCs in the corpus callosum, and found no significant difference in the number of OPCs between GamtGFP/GFP and control mice at P7, P14 or P21 (Fig. 3d). To determine if the lack of Gamt expression in mice affects myelination, immunostaining analysis for myelin basic protein (MBP) was performed. We found a significant decrease in MBP coverage in the corpus callosum at P21 (Fig. 3e and f). Moreover, we performed western blot analysis for myelin oligodendrocyte glycoprotein (MOG) expression in cerebellar extracts of GamtGFP/GFP and WT mice at P21, and found that GamtGFP/GFP mice exhibited reduced MOG expression compared to control (Fig. 3g and h). These results suggest that endogenously synthesized creatine is not involved in maintaining the OPC population in the adult corpus callosum, but plays a role in regulating oligodendrocyte differentiation and myelination.

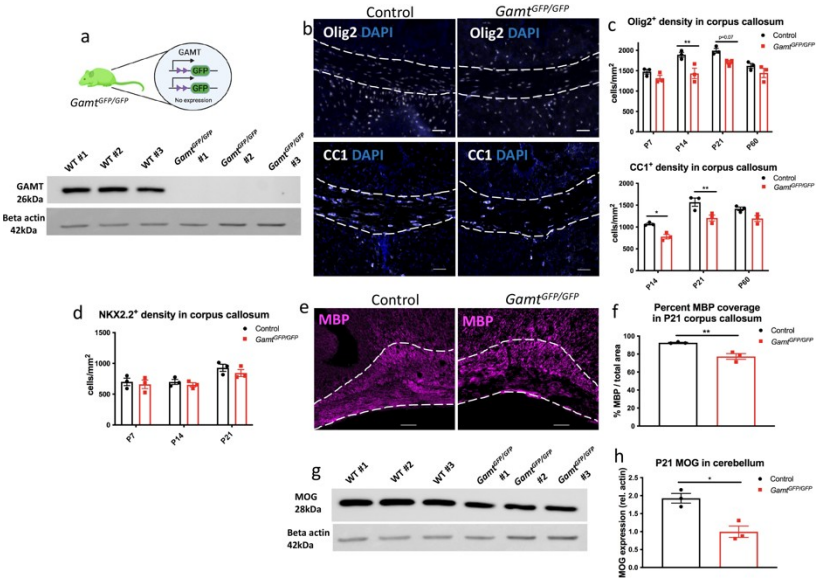

Fig 3. Deletion of Gamt results in reduced mature oligodendrocytes at P14 and P21 and a delay in developmental myelination. a) Diagram of GamtGFP/GFP knockout mouse (top) and confirmation of GAMT deletion by western blot (bottom). b) Immunostaining of control and GamtGFP/GFP for Olig2+ oligodendrocyte lineage cells and CC1+ oligodendrocytes in the corpus callosum at P14. c) Quantification showing total Olig2+ oligodendrocyte lineage cells at P14 (two-way ANOVA of genotype x age with Sidak's multiple comparisons; F (1, 4)=19.77, df=1 for genotype; p=0.01), CC1+ oligodendrocytes in the corpus callosum at P14 and P21 (two-way ANOVA with Sidak's multiple comparisons; F (1, 12)=33.86, df=1, p<0.0001), and d) NKX2.2+ OPC numbers (p=0.1, ns). e) Myelin basic protein (MBP) staining coverage at P21 is reduced in GamtGFP/GFP compared to controls. f) Quantification of MBP coverage at P21 (two-tailed t-test; t=4.721, df=4, p=0.009). g) Western blot analysis for myelin oligodendrocyte glycoprotein (MOG) expression in GamtGFP/GFP cerebellar extract at P21. h) Quantification of MOG expression in GamtGFP/GFP mice (two-tailed t-test; t=4.494, df=4, p=0.01). All data presented as mean±SEM with n=3 biological replicates. Scale bar is 50µm in b,e. Data presented with *p<0.05, **p<0.01.

4. Gamt deletion leads to altered energetics and reduced brain creatine kinase (BCK) in neurons in the cortex of adult mice. Defects in oligodendrocytes have long term effects on the health and

energetics of neurons since oligodendrocytes provide metabolic support, in addition to increasing axonal conduction velocity through myelin sheaths (Lee et al., 2012; Fünfschilling et al., 2012). AMPK is activated by increased levels of AMP and ADP stemming from a variety of cellular stresses in many cell types. Long term activation of AMPK leads to metabolic reprogramming within the brain including decreases in transcription, glucose synthesis and lipogenesis. Since creatine plays an important role in buffering ATP, and low ATP levels can lead to phosphorylation (activation) of AMP-kinase (AMPK) (Hardie et al., 2012), we examined AMPK signaling in the mouse cerebellum by Western blot analysis at P21 (Fig. 4a). We found that the GamtGFP/GFP mice displayed decreased total AMPK protein expression (Fig. 4b), and increased phospho-AMPK expression compared to control (Fig. 4c), suggesting a potential global shift in brain bioenergetics and metabolism in the absence of endogenously synthesized creatine.

Since oligodendrocytes are the only cells expressing Gamt at P21, we next asked if the loss endogenously synthesized creatine also affects neuronal bioenergetics in the adult CNS. Brain creatine kinase (BCK), which is essential for shuttling of high-energy phosphate group from phosphocreatine for ATP biogenesis, is mainly expressed in inhibitory neurons and astrocytes, but not in oligodendrocytes (Lowe et al., 2013), and is known to cooperate with AMPK to maintain energy homeostasis within cells (Ramírez Ríos et al., 2014). To determine if loss of GAMT affects BCK expression in neurons, immunostaining analysis of GamtGFP/GFP and control mice at P60 was performed (Fig. 4d). We found a significant decrease of BCK expression in NeuN+ neurons in the motor cortex of GamtGFP/GFP mice compared to control (Fig. 4e). However, no difference in overall number of neurons in the cortex was observed (Fig. 4f). Since BCK has been shown to be localized mainly in inhibitory neurons, we also assessed whether the loss of cerebral creatine affected GAD67+ inhibitory neuron numbers in mice. Immunostaining analysis revealed Gamt deletion had no effect on the total number of inhibitory neurons between (Fig. 4g). These

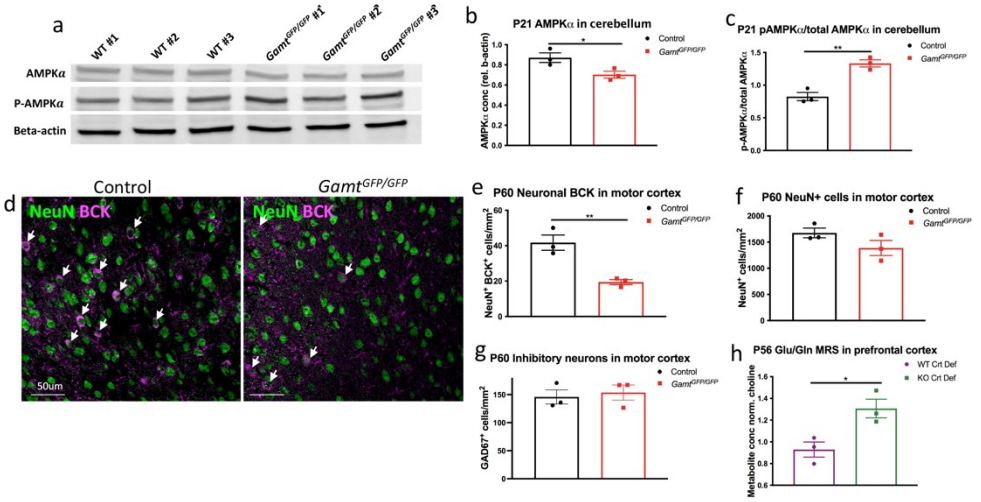

Fig 4. Loss of Gamt leads to activated AMPK signaling and reduced brain creatine kinase (BCK) in the cortex of adult mice. a) Western blot of cerebellar lysates for AMPK signaling in wildtype and GamtGFP/GFP knockout mouse at P21. b) Quantification of total AMPK (two-tailed t-test; t=2.884, df=4, p=0.045), and c) phosphorylated AMPK (two-tailed t-test; t=6.084, df=4, p=0.0037). d) Immunostaining of BCK and NeuN+ neurons in the motor cortex in controls and GamtGFP/GFP at P60. Quantification of e) BCK expression in neurons (two-tailed t-test; t=4.912, df=4, p=0.008), and f) total neurons in the motor cortex (p=0.16, ns). g) Quantification of GAD67+ inhibitory neurons in the motor cortex at P60 (p=0.695, ns). h) MRS analysis glutamate-glutamine ratio in GAMT KO on a creatine deficient diet compared to WT on creatine deficient diet at P56 (two-tailed t-test; t=3.417, df=4, p=0.027). All data presented as mean±SEM with n=3 biological replicates. Scale bar is 50µm in d. Data presented with *p<0.05, **p<0.01, ns=not significant.

results suggest that the cerebral creatine deficiency resulted in long term changes in cellular metabolism and bioenergetics, which may lead to neuronal dysregulation without affecting neuronal survival in the adult CNS. Indeed, MRS analysis of Gamt knockout mice exhibited increased glutamate/glutamine ratio compared to WT at P56, suggesting altered glutamatergic neurotransmission in the adult CNS (Fig. 4h).

5. Inducible knockout of Gamt in oligodendrocyte lineage cells leads to reduced oligodendrocytes and inefficient remyelination after demyelinating injury. We next investigated if Gamt expression in oligodendrocytes is required for remyelination. To this end, we crossed our Gamtfl/fl line with the PDGFRα-CreERT mouse line, and generated PDGFRα-CreERT;Gamtfl/fl to allow tamoxifen inducible knockout (iKO) of Gamt in oligodendrocyte lineage cells (Fig. 5a). To induce Gamt deletion in oligodendrocyte lineage cells, tamoxifen was injected intraperitoneally into mice at 10-11 weeks of age for four consecutive days, and focal experimental demyelination was then performed by lysolecithin injection into the mouse spinal cord ventral white matter. Sibling tamoxifen-injected Gamtfl/fl mice without PDGFRα-CreERT expression were used as controls. To confirm Gamt deletion, we examined the expression of GFP in the lesioned spinal cord of PDGFRα-CreERT;Gamtfl/fl iKO and control mice. At 5 days post lesion (dpl), when OPCs are expected to migrate and proliferate into lesions, we did not observe any GFP expression in or outside of the lesions of PDGFRα-CreERT;Gamtfl/fl iKO or control mice (Fig. 5b), suggesting that Gamt is not expressed at the OPC recruitment stage during remyelination. The lack of

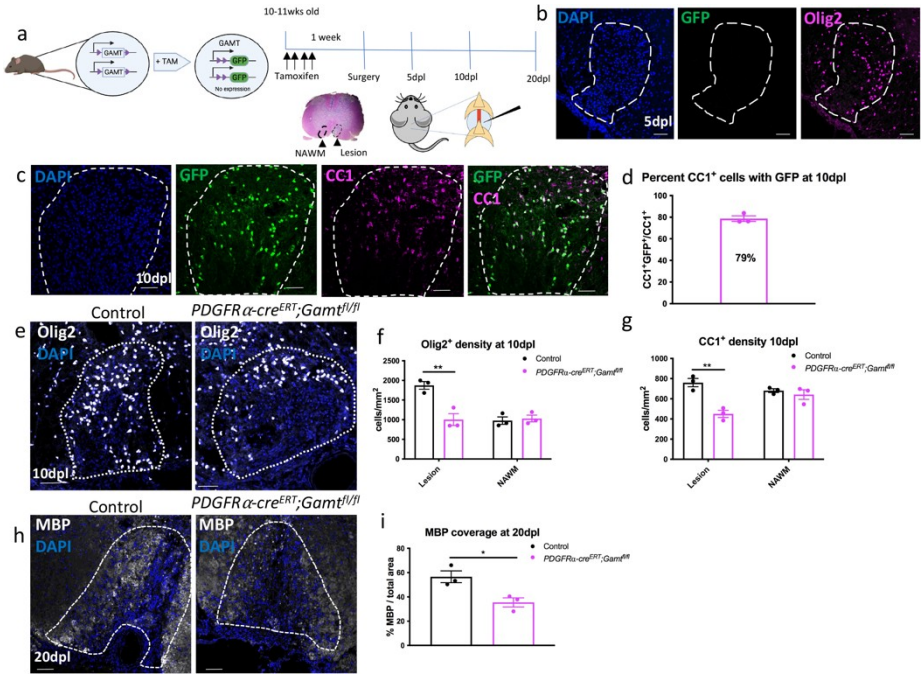

Fig 5. Deletion of Gamt from oligodendrocyte lineage cells leads to reduced mature oligodendrocytes and myelin coverage in lesions during remyelination. a) Diagram showing strategy to delete Gamt from oligodendrocyte lineage cells in PDGFRα-CreERT;Gamtfl/fl mice by i.p. injections of tamoxifen for four days, followed by lysolecithin spinal cord demyelination. b) No GFP expression was detected at 5 days post lesion (dpl). c) GFP expression in CC1+ mature oligodendrocytes in lesions at 10 dpl. d) Quantification shows GFP colocalization in 79 percent of mature oligodendrocytes in the lesions. e) Immunostaining of Olig2+ oligodendrocyte lineage cells in lesion of tamoxifen treated control and PDGFRα-CreERT;Gamtfl/fl mice. f) Quantification showing Olig2+ oligodendrocyte lineage cells (two-way ANOVA with Tukey's multiple comparisons; $F(1, 8)=13.76$, $df=1$, $p=0.006$) and g) CC1+ oligodendrocytes (two-way ANOVA with Tukey's multiple comparisons; $F(1, 8)=0.0016$, $df=1$, $p=0.0016$) in lesions of PDGFRα-CreERT;Gamtfl/fl iKO compared to control at 10 dpl. h) Immunostaining of myelin basic protein (MBP) at 20 dpl. i) Quantification showing (MBP) coverage in lesions of PDGFRα-CreERT;Gamtfl/fl iKO compared to control at 20 dpl (two-tailed t-test; $t=3.449$, $df=4$, $p=0.026$). All data presented as mean±SEM with n=3 biological replicates. Scale bar is 50µm in b,c,e,h. Data presented with *$p<0.05$, **$p<0.01$.

GFP expression also suggested that no mature oligodendrocytes that survived the lesion expressed GFP. However, at 10 dpl, when OPC are expected to have differentiated into oligodendrocytes, we found that GFP was expressed only in CC1+ oligodendrocytes in lesions and barely detectable outside of lesions (Fig. 5c). Quantification of GFP labeled oligodendrocytes showed approximately 79% of mature oligodendrocytes expressed GFP in lesions (Fig. 5d), suggesting that GFP+ oligodendrocytes were derived from OPCs that migrated into the lesion during remyelination. These results demonstrate the inducible GFP tagging approach using the PDGFRα-CreERT;Gamtfl/fl line allows for the tracking of newly regenerated oligodendrocytes in lesions, and the identification of Gamt deleted oligodendrocytes after demyelinating injury. To determine if tamoxifen induced Gamt deletion in oligodendrocyte lineage cells affected oligodendrocyte lineage cell progression in lesions, immunostaining analysis for oligodendrocyte lineage cell markers was performed. We detected a significant reduction of Olig2+ oligodendrocyte lineage cells and CC1+ oligodendrocytes in lesions in the PDGFRα-CreERT;Gamtfl/fl iKO compared to control at 10 dpl (Fig. 5e–g). Moreover, MBP coverage in the lesion, which is an indicator of remyelination, was significantly reduced at 20 dpl (Fig. 5h and i). These results suggest that creatine synthesis in oligodendrocytes is necessary for efficient oligodendrocyte maturation and remyelination.

6. Creatine or cyclocreatine supplemented recovery diet leads to increased mature oligodendrocytes and enhanced remyelination after cuprizone-mediated demyelination. Since 50% of creatine in human comes from diet, we next asked if dietary creatine is important in regulating the function of oligodendrocyte lineage cells with intact Gamt expression under demyelinating environment. To this end, wild type mice were fed a 0.2 percent cuprizone in either creatine deficient or standard rodent diet for five weeks, starting at eight weeks-old. (Fig. 6a). We found that mice on the creatine deficient diet displayed a significant reduction in Olig2+ oligodendrocyte lineage cells and CC1+ oligodendrocytes in the corpus callosum after five weeks of cuprizone treatment compared to those on regular rodent diet (Fig. 6b–d). Moreover, we observed a significant reduction in NKX2.2+ OPCs (Fig. 6e and f). These data suggest that the absence of dietary creatine leads to a greater loss of the entire oligodendrocyte lineage

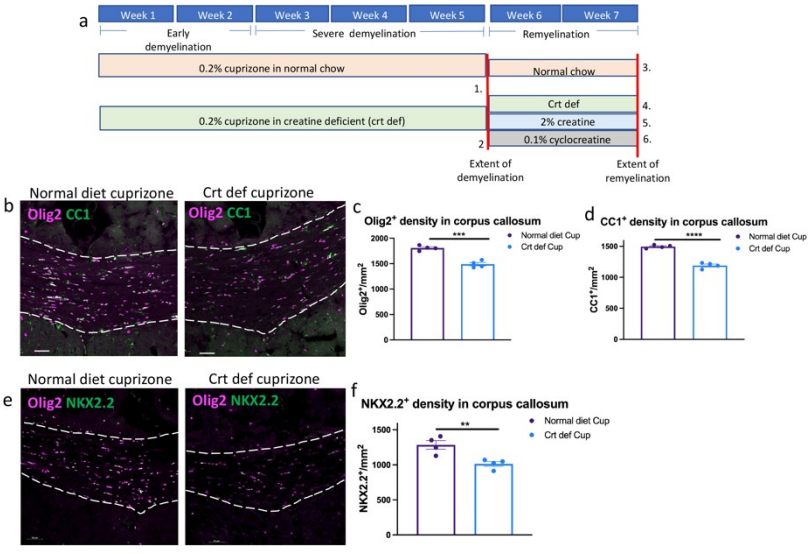

Fig 6. Cuprizone demyelination under creatine deficient diet results in greater loss of oligodendrocytes and oligodendrocyte precursor cells (OPC) in the corpus callosum. a) Diagram of cuprizone experiment and groups. b) Images of Olig2+CC1+ mature oligodendrocytes in the corpus callosum after five weeks of cuprizone with creatine deficient diet compared to cuprizone with normal diet. c) Quantification showing Olig2+ oligodendrocyte lineage cells (two-tailed t-test, t=7.717, df=6, p=0.0002) and d) CC1+ oligodendrocytes (two-tailed t-test; t=11.38, df=6, p<0.0001) in the corpus callosum. e) Images of Olig2+NKX2.2+ OPCs in corpus callosum after five weeks of cuprizone with creatine deficient diet compared to cuprizone with normal diet. f) Quantification showing NKX2.2+ OPCs in the corpus callosum (two-tailed t-test; t=3.819, df=6, p=0.009). All data presented as mean±SEM with n=4 biological replicates. Scale bar is 50µm in b,e. Data presented with *p<0.05, **p<0.01, ***p<0.001, ****p<0.0001.

during cuprizone intoxication, suggesting dietary creatine is protective against oligodendrocyte lineage cell loss and may be necessary to rapidly replenish cerebral creatine pools to lessen the effects of systemic cuprizone toxicity.

To determine if introduction of creatine into rodent diet enhances remyelination, a diet without cuprizone and containing 2% creatine or 0.1% cyclocreatine, a planar creatine analog with greater brain penetrance, were fed to mice for 2 weeks during the recovery period (Fig 6a) after 5 weeks of cuprizone demyelination. Control mice were fed a creatine deficient diet throughout the experiment. We found that both creatine and cyclocreatine fed mice displayed increased Olig2+CC1+ oligodendrocytes (Fig. 7a and b), and significantly greater Fluoromyelin staining (Fig. 7c and d) in the corpus callosum compared to control after two weeks of being on the recovery diet. Electron microscopy analysis revealed that creatine and cyclocreatine diets led to more remyelinated axons compared to control, and displayed lower g-ratios (Fig. 7e and f, g). These results suggest that dietary creatine significantly enhances CNS remyelination.

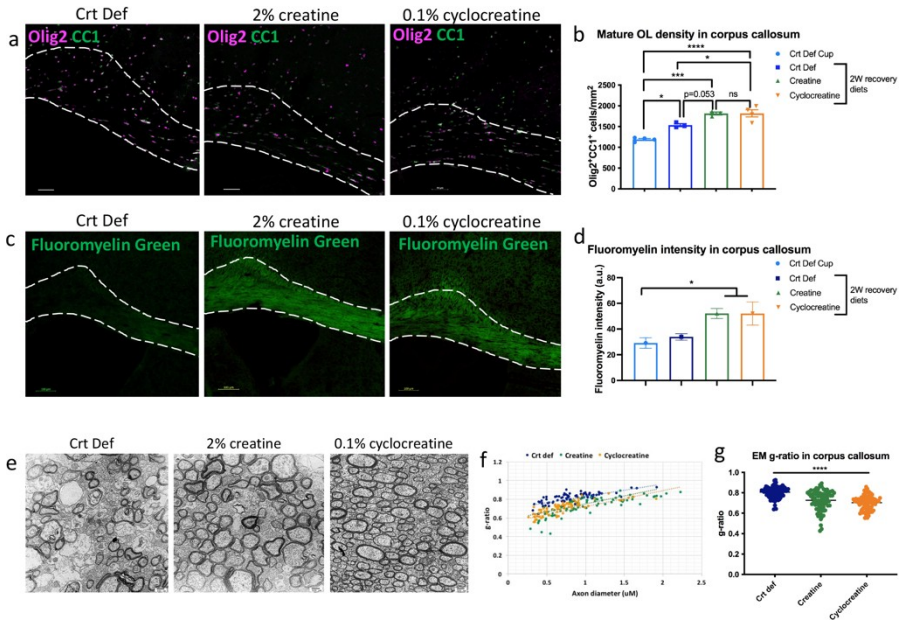

Fig 7. Creatine or cyclocreatine supplemented recovery diet increases mature oligodendrocytes and enhances remyelination. a) Images of Olig2+CC1+ mature oligodendrocytes in corpus callosum after two weeks of recovery diet containing either no creatine (Crt Def), 2% creatine, or 0.1% cyclocreatine. b) Quantification of CC1+ oligodendrocytes following two weeks of recovery diet (one-way ANOVA with Sidak's multiple comparisons; $F(3, 10)=29.58$, $df=13$, $p<0.0001$). c) Images of Fluoromyelin in corpus callosum after the different recovery diets. d) Quantification of Fluoromyelin intensity in the corpus callosum following two weeks of recovery diet (one-way ANOVA with Dunnett's multiple comparisons; $F(3, 11)=4.279$, $df=14$, $p=0.03$). e) EM images of axons in cross sections of corpus callosum from mice under the different recovery diets. Magnification x 5,000. f and g) G-ratio analysis of myelinated axons in the corpus callosum under the different recovery diets (one-way ANOVA with Tukey's multiple comparisons; $F(2, 237)=40.28$, $df=239$, $p<0.0001$). All data presented as mean±SEM with n=3-4 biological replicates in a-d. Representative EM analysis in e-g from n=1, 80 axons per animal. Scale bar is 100µm in a,c and 500nm in e. Data presented with *$p<0.05$, **$p<0.01$, ***$p<0.001$, ****$p<0.0001$, ns= not significant.

Single nuclear RNA-seq analysis reveals alteration in CNS associated genes in mice deficient in Gamt expression. To determine the effect of Gamt loss of function on the mouse CNS, dissociated nuclei from cortical tissues of Gamt KO and WT mice at P90 were obtained using the 10XGenomics chromium controller, cDNA libraries were generated and submitted for RNA-sequencing. Preliminary data indicates significant alteration in genes associated with neurons in the Gamt KO mice compare to control (Fig. 8). Since this was our first attempt, and involved two brains per mouse group, we plan to repeat this experiment and increase the number of mouse brains for analysis.

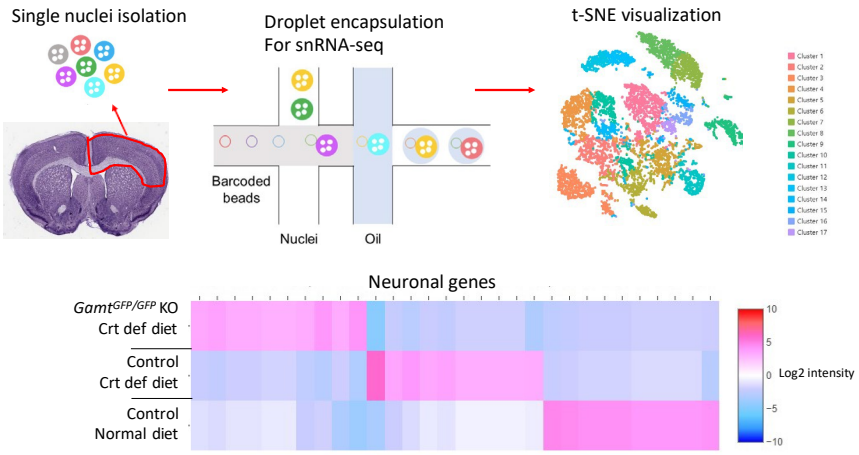

Fig 8. Single nuclear RNA-seq analysis of Gamt KO on creatine deficient diet, control mice on creatine deficient diet, and control mice on normal diet at P90.

What opportunities for training and professional development has the project provided?
If the project was not intended to provide training and professional development opportunities or there is nothing significant to report during this reporting period, state "Nothing to Report."

Nothing to Report

How were the results disseminated to communities of interest?
If there is nothing significant to report during this reporting period, state "Nothing to Report."

Nothing to Report

What do you plan to do during the next reporting period to accomplish the goals?

Nothing to Report

4. **IMPACT:** D*escribe distinctive contributions, major accomplishments, innovations, successes, or any change in practice or behavior that has come about as a result of the project relative to:*

What was the impact on the development of the principal discipline(s) of the project?
If there is nothing significant to report during this reporting period, state "Nothing to Report."

Our study indicates that oligodendrocytes are the major cell type that produces creatine in the adult brain. This study demonstrates the importance of creatine in oligodendrocyte development and remyelination, and suggests creatine synthesis in oligodendrocytes is a critical regulator of remyelination, which is highly relevant to multiple sclerosis repair.

What was the impact on other disciplines?
If there is nothing significant to report during this reporting period, state "Nothing to Report."

This study suggests loss of creatine in oligodendrocytes may be a contributor to neurological behaivoral abnormality in cerebral creatine deficiency syndrome.

What was the impact on technology transfer?
If there is nothing significant to report during this reporting period, state "Nothing to Report."

Nothing to Report

What was the impact on society beyond science and technology?
If there is nothing significant to report during this reporting period, state "Nothing to Report."

Nothing to Report

5. **CHANGES/PROBLEMS:** *The PD/PI is reminded that the recipient organization is required to obtain prior written approval from the awarding agency grants official whenever there are significant changes in the project or its direction. If not previously reported in writing, provide the following additional information or state, "Nothing to Report," if applicable:*

Changes in approach and reasons for change
Describe any changes in approach during the reporting period and reasons for these changes. Remember that significant changes in objectives and scope require prior approval of the agency.

Nothing to Report

Actual or anticipated problems or delays and actions or plans to resolve them
Describe problems or delays encountered during the reporting period and actions or plans to resolve them.

The transgenic mice were difficult to breed. It took some time to obtain sufficient offsprings to perform our experiments. It was difficult to obtain enough tissues for electron microspy analysis, and we were unable to use the electron microscope at Georgetown Univeristy because it was under repair. Our lab was also affected by the covid pandemic, and this slowed down productivity.

Changes that had a significant impact on expenditures

Nothing to Report

Significant changes in use or care of human subjects, vertebrate animals, biohazards, and/or select agents
Describe significant deviations, unexpected outcomes, or changes in approved protocols for the use or care of human subjects, vertebrate animals, biohazards, and/or select agents during the reporting period. If required, were these changes approved by the applicable institution committee (or

equivalent) and reported to the agency? Also specify the applicable Institutional Review Board/Institutional Animal Care and Use Committee approval dates.

Significant changes in use or care of human subjects

N/A

Significant changes in use or care of vertebrate animals

Nothing to Report

Significant changes in use of biohazards and/or select agents

Nothing to Report

6. **PRODUCTS:** *List any products resulting from the project during the reporting period. If there is nothing to report under a particular item, state "Nothing to Report."*

- **Publications, conference papers, and presentations**
  Report only the major publication(s) resulting from the work under this award.

  Journal publications.

  Manuscript containing data presented in this report are currently under revision in Journal of Neuroscience. Acknowledgement of federal support for this project was provided in the manuscript.

  Books or other non-periodical, one-time publications.

  N/A

  Other publications, conference papers and presentations.

  Nothing to Report

- **Website(s) or other Internet site(s)**

  N/A

- **Technologies or techniques**

  N/A

- **Inventions, patent applications, and/or licenses**

N/A

- **Other Products**

N/A

7. PARTICIPANTS & OTHER COLLABORATING ORGANIZATIONS

What individuals have worked on the project?
Provide the following information for: (1) PDs/PIs; and (2) each person who has worked at least one person month per year on the project during the reporting period, regardless of the source of compensation (a person month equals approximately 160 hours of effort). If information is unchanged from a previous submission, provide the name only and indicate "no change".

Name:	*Jeffrey Huang*
Project Role:	*PI*
Researcher Identifier (e.g. ORCID ID):	*huangjeffrey*
Nearest person month worked:	*36*
Contribution to Project:	*Oversaw the study*
Name:	*Lauren Rosko*
Project Role:	*Graduate Student*
Researcher Identifier (e.g. ORCID ID):	*N/A*
Nearest person month worked:	36
Contribution to Project:	*Ms. Rosko has performed all major experiments described*

Has there been a change in the active other support of the PD/PI(s) or senior/key personnel since the last reporting period?

N/A

What other organizations were involved as partners?
If there is nothing significant to report during this reporting period, state "Nothing to Report."

N/A

8. SPECIAL REPORTING REQUIREMENTS

N/A

9. **APPENDICES:** *Attach all appendices that contain information that supplements, clarifies or supports the text. Examples include original copies of journal articles, reprints of manuscripts and abstracts, a curriculum vitae, patent applications, study questionnaires, and surveys, etc.*

N/A

The Journal of Neuroscience

https://jneurosci.msubmit.net

Creatine synthesis through guanidinoacetate methyltransferase (Gamt) regulates the timing of oligodendrocyte myelination

Jeffrey Huang, Georgetown University
Lauren Rosko, Georgetown University
Tyler Gentile, Georgetown University
Victoria Smith, Georgetown University
George Melchor, Georgetown University
Jingwen Hu, Georgetown University
Chris Albanese, Georgetown University Medical Center
Yichien Lee, Georgetown University Medical Center
Olga Rodriguez, Georgetown University Medical Center
Nataliia Schults, Georgetown University

Commercial Interest:

Creatine synthesis through guanidinoacetate methyltransferase (*Gamt*) regulates the timing of oligodendrocyte myelination

Abbreviated Title: Endogenous creatine regulates CNS myelination

Lauren M. Rosko[1,2], Tyler Gentile[1], Victoria N. Smith[1], George S. Melchor[1,2], Jingwen Hu[1], Chris Albanese[3], Yichien Lee[3], Olga Rodriguez[3], Nataliia V. Shults[1], Jeffrey K. Huang[1,2,*]

[1]Department of Biology, Georgetown University, 37th and O St., NW, Washington, DC 20057

[2]Interdisciplinary Program in Neuroscience, Georgetown University, Washington DC, USA 20057

[3]Department of Oncology, Georgetown University Medical Center, Washington DC, USA 20057

[*]Corresponding author: jeffrey.huang@georgetown.edu

Total Pages: 32

Number of Figures: 8

Number of Extended Data Figures: 2

Word count:

Abstract: 248

Introduction: 523

Discussion: 858

COMPETING INTERESTS

The authors declare no competing financial interests

ACKNOWLEDGEMENTS

This study was supported by the Department of Defense CDMRP Investigator-Initiated Research Award (W81XWH-17-1-0268) and National Multiple Sclerosis Society Harry Weaver Neuroscience Scholar Award (JF-1806-31381) to J.K.H, and the National Center For Advancing Translational Sciences of the National Institutes of Health (TL1TR001431) training fellowship to L.M.R. We thank members of the Huang lab for comments on this project, and the Preclinical Imaging Research Laboratory at Georgetown University Medical Center for mouse MRS imaging. We also thank Robert Miller and Molly Karl at George Washington University for EM training to N.V.S.

AUTHOR CONTRIBUTIONS

J.K.H. and L.M.R. designed the study. L.M.R. performed all mouse experiments and data analysis. T.G., V.N.S., G.S.M., J.H. contributed to mouse experiments and data analysis. N.V.S. performed electron microscopy. Y.L., O.R., C.A. conducted magnetic resonance spectroscopy. L.M.R. and J.K.H. wrote the manuscript with contributions from all authors. J.K.H. oversaw the study.

ABSTRACT

Cerebral creatine deficiency syndrome (CCDS) is an inborn error of metabolism characterized by intellectual delays, seizures, and autistic-like behavior. Exactly how endogenously synthesized creatine regulates central nervous system (CNS) function remains poorly understood. Here, magnetic resonance spectroscopy (MRS) of adult mouse brains from both sexes revealed creatine synthesis is dependent on the expression of the enzyme guanidinoacetate methyltransferase (GAMT). To identify *Gamt*-expressed cells, and the role of *Gamt* in postnatal CNS development, we generated a mouse line by knocking-in a green fluorescent protein (GFP) that becomes expressed upon excision of *Gamt*. We found that *Gamt* is strongly expressed in mature oligodendrocytes during active myelination in the postnatal CNS. Homozygous deletion of *Gamt* resulted in significantly reduced mature oligodendrocytes and delayed myelination in the corpus callosum. Moreover, *Gamt* deletion resulted in altered AMPK signaling in the brain, and reduced brain creatine kinase expression in cortical neurons. Experimental demyelination of mice after tamoxifen induced conditional deletion of *Gamt* in oligodendrocyte lineage cells resulted in reduced mature oligodendrocytes and myelin coverage in lesions. Moreover, creatine and cyclocreatine supplementation can enhance remyelination after demyelination. Our results suggest endogenously synthesized creatine controls the bioenergetic demand required for the timely maturation of oligodendrocytes during postnatal CNS development, and that delayed myelination and altered energetic metabolism in the CNS through the disruption of creatine synthesis in oligodendrocytes might contribute to CCDS.

SIGNIFCANCE STATEMENT

Cerebral creatine deficiency syndrome (CCDS) is a rare disease of inborn errors in metabolism, which is characterized by intellectual delays, seizures, and autism-like behavior. We found that oligodendrocytes are the main source of endogenously synthesized creatine in the adult CNS, and the loss of endogenously synthesized creatine led to delayed myelination and altered neuronal metabolism. Our study suggests impaired cerebral creatine synthesis affects timing of myelination, which may have widespread impact on brain bioenergetics and metabolism.

INTRODUCTION

The creatine-phosphocreatine shuttle plays an essential role in energy metabolism (Wyss et al., 2007). During periods of high energetic demand, creatine kinases catalyze the transfer of the high-energy phosphate group in phosphocreatine to ADP, allowing for the rapid generation/regeneration of ATP, thereby maintaining the energetic supply required for cellular function (Wyss et al., 2007). About half of our daily creatine is derived from diet. The other half is endogenously synthesized by the conversion of glycine and arginine into guanidinoacetate through the enzyme arginine:glycine amidinotransferase (AGAT), and the subsequent transformation of guanidinoacetate into creatine through the enzyme guanidinoacetate methyltransferase (GAMT). Creatine can then be converted to phosphocreatine and utilized by cells endogenously or transferred to other cells through the creatine transporter, SLC6A8. Humans with mutations in *AGAT*, *GAMT,* or *SLC6A8*, display cerebral creatine deficiency syndromes (CCDS), which are rare diseases that are characterized by the disruption of the

synthesis or transfer of creatine (Wyss and Kaddurah-Daouk, 2000; Braissant et al., 2011). If left untreated, children with CCDS can present with severe intellectual disabilities, seizures, developmental delays, autistic-like behaviors and movement disorders, suggesting that the brain is particularly vulnerable to creatine deficiency (Giusti et al., 2019).

Previous studies suggest that two main waves of creatine synthesis occur during rodent CNS development: one from mitotic cells of the subventricular zone and the external layer of the cerebellum, and the second from oligodendrocytes starting at two weeks old and continuing into adulthood (Tachikawa et al., 2018; Tachikawa et al., 2004; Baker et al., 2021). The profound increase in postnatal *Gamt* expression coincides with active CNS myelination (Sturrock, 1980), and suggests oligodendrocytes may be the major source of endogenous creatine within the postnatal brain. During active myelination, oligodendrocytes require a tremendous amount of energy for myelination. An estimated 3.24×10^{23} ATP molecules are required to synthesize one gram of myelin (Harris and Attwell, 2012), and disruption of oligodendrocyte energetic metabolism, i.e. from hypoglycemia, causes a significant delay in CNS myelination (Yan and Rivkees, 2006; Rinholm et al., 2011). We have previously found that creatine protects oligodendrocytes from mitochondrial-mediated apoptosis during injury, and promotes remyelination (Chamberlain et al., 2017). However, whether endogenously synthesized creatine is necessary for developmental myelination or remyelination remains unclear. Since myelination is an energetically demanding process, we hypothesized that

oligodendrocyte-derived creatine is required for developmental myelination and remyelination.

Here, we show that GAMT is the primary enzyme responsible for endogenously synthesized creatine in the mouse CNS. To track creatine production in the CNS, we developed a novel transgenic floxed mouse line that expresses green fluorescent protein (GFP) upon the conditional excision of *Gamt*, to allow the tracking of cells producing creatine, and for the analysis of *Gamt* loss of function in the mouse CNS. We found that oligodendrocytes are the only cells expressing GFP in the adult CNS, and that *Gamt* deletion resulted in delayed myelination and remyelination. Additionally, *Gamt* deletion also led to altered neuronal bioenergetics in the adult brain. Our results suggest oligodendrocytes are the major producers of creatine in the adult CNS, and that oligodendrocyte dysfunction through the loss of *Gamt* expression may contribute to the CNS pathophysiology associated with CCDS.

MATERIALS AND METHODS

Mice. Mice of both sexes were used for each experiment. *GAMT*$^{-/+}$ mice for magnetic resonance spectroscopy (MRS) were a kind gift from Dr. Dirk Isbrandt (University of Cologne). Floxed *Gamt (Gamt*$^{fl/fl}$*)* line was engineered by Cyagen Biosciences where a linearized vector was electroporated into embryonic stem cells (C57BL/6). After confirming clones by Southern Blotting, a chimera was produced by blastocyst microinjection. Floxed *Gamt* line was bred with Tg(CMV-cre)1Cgn (Stock 006054) line from Jackson Laboratory to generate a heterozygous mutant (*Gamt*$^{GFP/+}$) and knockout

mutant (*Gamt*$^{GFP/GFP}$). Tg(Pdgfra-cre/ERT)467Dbe (stock 018280) from Jackson was used to generate inducible removal of *Gamt* from oligodendrocytes (OL *Gamt* iKO). Wildtype C57BL/6J (Stock 000664) mice were also obtained from Jackson laboratory. Mice were maintained on a 12hr light/dark cycle with food and water *ad libitum*. All experiments were performed according to the protocol approved by the Institutional Animal Care and Use Committee at Georgetown University.

Magnetic Resonance Spectroscopy (MRS). Animals underwent small animal imaging at the Preclinical Imaging Research Laboratory and the Center for Translational Imaging at Georgetown-Lombardi University Medical Center in a Bruker 7T/20 Magnetic Resonance Imager spectrometer incorporating Bruker AVANCE III electronics and ParaVision software version 5.1. Briefly, animals were anesthetized (1.5% isoflurane in a gas mixture of 30% oxygen and 70% nitrous oxide) and placed on a custom-manufactured (ASI Instruments, Warren, MI) stereotaxic device with built-in temperature and cardio-respiratory monitoring engineered to fit a 25 mm Bruker mouse volume coil, as previously described (Albanese et al., 2013,Sirajuddin et al., 2012,Fricke et al., 2006). A T2-weighted two-dimensional anatomical locator scan was run followed by a volume-localized PRESS sequence with the following parameters: TE: 20 ms, TR: 2500 ms, averages: 1024, spectral width of 4 kHz, and 512 k complex data points and 6 Hz line broadening, using a single voxel localized on the frontal cortex. All *in vivo* peak integrated areas were analyzed using Bruker's "TOPSPIN" software to assess relative differences in tissue chemistry, as described previously (Albanese et al., 2013;

Sirajuddin et al., 2012; Fricke et al., 2006). The concentrations of metabolites were normalized to choline.

Immunohistochemistry (IHC). Mice were perfused with 4% PFA (Sigma) in PBS. Spinal cords and brains were removed and post fixed in PFA followed by 20% sucrose overnight. Brains were further cryoprotected in 30% sucrose before freezing in optimal cutting temperature medium (Sakura) on dry ice, then stored at -80°C. Twelve micron sections of spinal cord or brain were sectioned on a cryostat and mounted on SuperFrostPlus slides. Slides were incubated in blocking solution (10% goat serum, 1% donkey serum, 0.25% triton in TBS) for 1hr at RT. Mouse antibodies used an extra 1hr of mouse-on-mouse blocking reagent (Vector laboratories). Primary and secondary antibodies were diluted in blocking solutions. Primary antibodies for IHC were as follows: chicken GFP (1:2000, Thermo Fisher Cat# PA1-86341, RRID:AB_931091), mouse GFAP (1:500, Sigma-Aldrich Cat# G6171, RRID:AB_1840893), rabbit Iba1 (1:1000, FUJIFILM Wako Shibayagi Cat# 019-19741, RRID:AB_839504), mouse NeuN (1:200, Millipore Cat# MAB377, RRID:AB_2298772), rabbit Olig2 (1:300, Millipore Cat# MABN50, RRID:AB_10807410), ms CC1 (1:200; Millipore Cat# OP80, RRID:AB_2057371), rat myelin basic protein (1:500, Millipore Cat# MAB386, RRID:AB_94975), mouse NKX2.2 (1:100, DSHB Cat# 74.5A5, RRID:AB_531794), rabbit BCAS1 (1:1000, Synaptic Systems Cat# 445 003, RRID:AB_2864793), rabbit brain creatine kinase (1:200, Abcam Cat# ab2117, RRID:AB_2080889) and mouse Nestin (1:500, BD Biosciences Cat# 611658, RRID:AB_399176). Antigen retrieval

pretreatment was used for examining GFP expression. To use the 488 (green) channel in IHC without GFP interference, no antigen retrieval was used on slides.

Western blot. Tissues were dissected from mice at various postnatal time points, flash frozen and stored at -80°C. Tissues were digested in RIPA lysis buffer (Millipore), separated by SDS-PAGE and immunoblotted with antibodies: guinea pig GAMT (1:500; Frontier Inst), rabbit AMPKα1 (1:1000; Abcam), rabbit p-AMPKα (1:1000; Cell signaling), mouse MOG (1:500; Santa Cruz), and rabbit β-actin (1:5k; Abcam). Proteins were detected using horseradish peroxidase-conjugated secondary antibodies and Pierce ECL Western blotting substrate. Membrane stripping was done with mild stripping solution (ThermoFisher) and efficient stripping, or no signal, was confirmed by incubating with secondary antibody and re-incubating with ECL.

TUNEL. Slides were dried for 1hr before staining with Click-iT Plus TUNEL assay for *in situ* apoptosis detection (Fisher; C10618). Steps followed the manufacturer's instructions. A positive control slide was treated with DNase I.

Tamoxifen. 4-hydroxytamoxifen (Sigma) was diluted in 100% ethanol and then diluted in peanut oil to a final concentration of 4mg/mL. At 9-11 weeks of age, tamoxifen injections (1mg) were administered by IP consecutively for four days ending five days before focal demyelination surgery.

Spinal cord demyelination. Focal demyelination was induced by injection of 1.0% lysolecithin (Sigma) diluted in sterile PBS into ventral funiculus. Mice were euthanized for analysis at 5, 10 or 20 days after surgery.

Cuprizone and special diets. All animals were fed a creatine deficient amino acid diet (Crt def diet; Envigo; TD.01084) unless otherwise specified. Demyelination was induced in eight-week-old male and female mice by adding 0.2% cuprizone (Bis(cyclohexanone)oxaldihydrazone) into normal chow (LabDiet 5053) or crt def diet for 5 weeks. Cuprizone diet was replaced every three days to prevent stability concerns. All recovery diets used TD.01084 and added creatine or cyclocreatine (Sigma). Recovery diets after cuprizone were one of the following: Normal chow, crt def diet, 2% creatine, or 0.1% cyclocreatine. Animals were weighed once every two days to ensure animals did not lose more than ten percent body weight.

Electron microscopy. Animals were perfused with EM fixation solution (4% PFA, 2% glutaraldehyde, 0.1M sodium cacodylate buffer). Tissues were postfixed with 1% osmium tetroxide, and embedded in EmBed812. Ultrathin sections (70 nm) were poststained with uranyl acetate and lead citrate and examined in the Hitachi H7600 transmission electron microscope at 80 kV located at Georgetown University. Digital electron micrographs were recorded with the TIA software (FEI). Morphometric analysis was performed under blinded conditions by systematic uniform random sampling using 25 randomly selected images. ImageJ software (NIH) was used to obtain axon diameter measurements from EM images taken at 5000X magnification and g-ratios using the

freehand selection tool (>80 axons per animal; n=1). For g-ratios, the inner myelin sheath diameter was divided by the outer myelin sheath diameter.

Experimental design and statistical analyses. Images were collected on a Zeiss LSM 800 completed system confocal imager. Quantification of immunostaining was done by 1 or 2 blinded investigators using the ImageJ cell counter manually. For corpus callosum imaging, one medial and two lateral images of corpus callosum and cingulum were taken from 3-4 sections per slide (n=3). For spinal cord demyelinating lesions, the lesion was located by visualizing the accumulation of Hoechst-positive nuclei within the ventral white matter. A minimum of three lesion sections from three mice were analyzed for cell density. For cuprizone, three regions from four sections per animal were analyzed (n=4). Density per square millimeter was calculated in Microsoft Excel as previously described in Chamberlain et. al, 2017. All statistics were performed using Prism. Data are expressed as mean±SEM. Comparisons were analyzed by two-way ANOVA with Sidak's multiple comparison test, one-way ANOVA with Tukey's multiple comparison test or two-tailed t-test. Statistical significance is reported as *p≤0.05, **p≤ 0.01, ***p≤ 0.001, ****p≤ 0.0001.

RESULTS

Endogenously synthesized creatine supplies cerebral creatine and is dependent on *Gamt* expression.

Previous studies from our lab demonstrated that *Gamt* loss-of-function in mice impairs remyelination following experimental demyelinating injury (Chamberlain et al., 2017).

However, these mice did not display obvious myelination defects or developmental abnormalities, suggesting that cerebral creatine levels may not have been disrupted during development. To determine if cerebral creatine is detectable in the absence of *Gamt* expression, we performed ^{1}H-magnetic resonance spectroscopy (MRS) analysis in the prefrontal cortex of eight-week old *Gamt* knockout (KO) (Fig. **1a**) and wild-type (WT) mice (Fig. **1b**). MRS is a specialized, non-invasive imaging-based technique that enables the metabolic profiling of tissues *in vivo*. The level of creatine was also compared to the levels of glutamate/glutamine, myo-inositol, taurine, choline and N-acetylaspartate in the mouse prefrontal cortex (Fig. **1c**). We found that the KO mice on a standard rodent diet displayed measurable, but significantly lower creatine levels in the brain compared to WT (Fig. **1d**), suggesting that dietary creatine can partially compensate for cerebral creatine levels when GAMT is missing. MRS analysis was also performed on KO and WT mice on a creatine deficient diet. We found that WT mice on creatine deficient diet displayed similar creatine levels as those on standard diet. By contrast, *Gamt* KO mice on creatine deficient diet displayed undetectable creatine levels in the prefrontal cortex (Fig. **1d**). These data suggest that endogenously synthesized creatine can supply adequate cerebral creatine in the absence of dietary creatine, and that GAMT is the main enzyme responsible for creatine synthesis in the mouse brain. Moreover, our data also suggest that dietary creatine can supply cerebral creatine in the absence of *Gamt* expression in mice, providing an explanation for the lack of obvious myelination impairment in our previous study (Chamberlain et al., 2017). To examine the effect of *Gamt* deletion on postnatal CNS development, following studies were performed on mice on creatine deficient diet.

Gamt knock-in reporter mouse line reveals mature oligodendrocytes are the major producers of creatine in the postnatal CNS.

Gamt expression does not begin until very late in rodent embryogenesis and is regionally limited before birth (Braissant et al., 2005). As rodent development progresses, *Gamt* spatiotemporal expression changes drastically (Tachikawa et al., 2004; Braissant et al., 2005). To more effectively track the expression of *Gamt* and identify the cell populations that synthesize creatine endogenously, we developed a transgenic mouse model that expresses a green fluorescent protein (GFP) reporter upon the conditional excision of *Gamt*. This mouse line ($Gamt^{fl/fl}$) contains LoxP sites flanking exons 2-6 of the *Gamt* gene (Fig. **2a** and Extended Data Fig. **2-1**). To delete *Gamt* developmentally and in all tissues, $Gamt^{fl/fl}$ were crossed with a cytomegalovirus Cre recombinase-expressing mouse line (*CMV-Cre*). Heterozygous mice containing one copy of *Gamt* ($Gamt^{GFP/+}$) were used to track CNS cell populations that synthesize creatine while the mice with homozygous deletion ($Gamt^{GFP/GFP}$) were used for *Gamt* loss-of-function analysis. Controls are $Gamt^{fl/fl}$ without Cre recombinase. Immunohistochemistry was performed to co-localize GFP expression within CNS cell types in the cortex from postnatal (P) day P0 until P60.

We observed low, but widespread GFP expression in neuroblasts/neural stem cells (Fig. **2b**), neurons (Fig. **2c**), oligodendrocytes (Fig. **2d**), and astrocytes (Fig. **2e**) at P0 and P7, which supports previously published *Gamt* expression data (Tachikawa et al., 2018). However, by P14, when large-scale active developmental myelination is

occurring (Sturrock, 1980), this wide-spread expression was no longer observed, and GFP expression appeared to be restricted to distinctive cell populations in the CNS. We found that GFP was not expressed in GFAP$^+$ astrocytes (Fig. **2f**), Iba1$^+$ microglia (Fig. **2g**), or NeuN$^+$ neurons (Fig. **2h**), but was strongly expressed in Olig2$^+$ oligodendrocyte lineage cells in corpus callosum (Fig. **2i**). To further determine when endogenous creatine synthesis occurs during oligodendrocyte lineage cell progression, immunostaining analysis for GFP expression and NKX2.2$^+$ OPCs, BCAS1$^+$ premyelinating oligodendrocytes, and CC1$^+$ mature oligodendrocytes was performed. We found that GFP was undetectable in OPCs (Fig. **2j**), expressed in few premyelinating oligodendrocytes (Fig. **2k**), and abundantly expressed in mature oligodendrocytes (Fig. **2l**). Quantification revealed GFP expression in approximately 17% of premyelinating oligodendrocytes and 95% of mature oligodendrocytes (Fig. **2m**). These results suggest that during active myelination, endogenous creatine synthesis in the adult CNS occurs exclusively in oligodendrocytes during their maturation.

Gamt deletion leads to reduced mature oligodendrocyte survival and delayed myelination.

We next determined the impact of *Gamt* loss-of-function on CNS myelination in homozygous *Gamt*$^{GFP/GFP}$, and control *Gamt*$^{fl/fl}$ (WT) mice. To confirm *Gamt* deletion, western blot analysis for GAMT protein expression in brain extracts of WT and *Gamt*$^{GFP/GFP}$ mice at P21 were performed. We observed a complete loss of GAMT expression (26 kDa) in *Gamt*$^{GFP/GFP}$ mice compared to control, indicating *Gamt* was effectively deleted in the CNS of *Gamt*$^{GFP/GFP}$ mice (Fig. **3a**). Next, we compared the

total number of oligodendrocyte lineage cells in the corpus callosum in *Gamt*$^{GFP/GFP}$ and control mice by immunostaining analysis (Fig. **3b**). We observed a significant reduction of total Olig2^{+} oligodendrocyte lineage cell numbers at P14 and a trending decrease at P21 in *Gamt*$^{GFP/GFP}$ mice compared to control (Fig. **3c;** top). Moreover, we observed a significant decrease of CC1^{+} mature oligodendrocytes in *Gamt*$^{GFP/GFP}$ mice at P14 and P21 (Fig **3c;** bottom). However, this reduction in total number of oligodendrocytes was no longer significant by P60 (Fig **3c**). We also examined the number of NKX2.2 OPCs in the corpus callosum, and found no significant difference in the number of OPCs between *Gamt*$^{GFP/GFP}$ and control mice at P7, P14 or P21 (Fig. **3d**). To determine if the lack of *Gamt* expression in mice affects myelination, immunostaining analysis for myelin basic protein (MBP) was performed. We found a significant decrease in MBP coverage in the corpus callosum at P21 (Fig. **3e** and **f**). Moreover, we performed western blot analysis for myelin oligodendrocyte glycoprotein (MOG) expression in cerebellar extracts of *Gamt*$^{GFP/GFP}$ and WT mice at P21, and found that *Gamt*$^{GFP/GFP}$ mice exhibited reduced MOG expression compared to control (Fig. **3g** and **h**). These results suggest that endogenously synthesized creatine is not involved in maintaining the OPC population in the adult corpus callosum, but plays a role in regulating oligodendrocyte differentiation and myelination. However, since the number of oligodendrocytes in *Gamt*$^{GFP/GFP}$ mice eventually catches up to control levels by adulthood, our results suggest that endogenous creatine synthesis may be necessary to ensure oligodendrocyte differentiation and myelination occurs in a timely manner in the postnatal CNS.

To investigate whether the reduction in mature oligodendrocytes was driven by decreased proliferation or increased cell death, we performed immunohistochemistry at P14 and P21. First, we conducted a TUNEL assay for apoptosis, and found increased TUNEL staining in the corpus callosum in *Gamt*$^{GFP/GFP}$ compared to control at P14 and P21 (Fig. **4a** and **b**). Moreover, we observed that most of the dying cells were Olig2^{+} oligodendrocyte lineage cells (Fig. **4c**). Interestingly, we found that the TUNEL positive cells did not colocalize with markers of OPCs or mature oligodendrocytes in the *Gamt*$^{GFP/GFP}$ mice, but appeared to colocalize with BCAS1 (Fard et al., 2017), suggesting that premyelinating oligodendrocytes undergoes cell death in the absence of creatine (Fig. **4d** and **e**). Next, we stained for Ki67 to examine the effect of *Gamt* loss of function on cell proliferation, and found no difference in proliferation in the corpus callosum between *Gamt*$^{GFP/GFP}$ and control mice at P14 or P21 (Fig. **4f**). Since myelination depends on lipogenesis, we also examined the expression of fatty acid synthase (FASN) in the corpus callosum (Dimas et al., 2019). We observed complete colocalization between FASN and mature oligodendrocyte marker, CC1, and unsurprisingly, decreased FASN expression in our *Gamt*$^{GFP/GFP}$ model compared to WT, indicating reduced oligodendrocyte lipogenesis in the corpus callosum (Extended Data Fig. **4-1**). These results suggest that endogenously synthesized creatine may be necessary to provide the energy necessary to promote the transition of premyelinating oligodendrocytes to mature oligodendrocytes, and that premyelinating oligodendrocytes are vulnerable to apoptosis in the absence of endogenously synthesized creatine.

Gamt deletion leads to altered energetics and reduced brain creatine kinase (BCK) in neurons in the cortex of adult mice.

Defects in oligodendrocytes have long term effects on the health and energetics of neurons since oligodendrocytes provide metabolic support, in addition to increasing axonal conduction velocity through myelin sheaths (Lee et al., 2012; Fünfschilling et al., 2012). AMPK is activated by increased levels of AMP and ADP stemming from a variety of cellular stresses in many cell types. Long term activation of AMPK leads to metabolic reprogramming within the brain including decreases in transcription, glucose synthesis and lipogenesis. Since creatine plays an important role in buffering ATP, and low ATP levels can lead to phosphorylation (activation) of AMP-kinase (AMPK) (Hardie et al., 2012), we examined AMPK signaling in the mouse cerebellum by Western blot analysis at P21 (Fig. **5a**). We found that the *Gamt*$^{GFP/GFP}$ mice displayed decreased total AMPK protein expression (Fig. **5b**), and increased phospho-AMPK expression compared to control (Fig. **5c**), suggesting a potential global shift in brain bioenergetics and metabolism in the absence of endogenously synthesized creatine.

Since oligodendrocytes are the only cells expressing *Gamt* at P21, we next asked if the loss endogenously synthesized creatine also affects neuronal bioenergetics in the adult CNS. Brain creatine kinase (BCK), which is essential for shuttling of high-energy phosphate group from phosphocreatine for ATP biogenesis, is mainly expressed in inhibitory neurons and astrocytes, but not in oligodendrocytes (Lowe et al., 2013), and is known to cooperate with AMPK to maintain energy homeostasis within cells (Ramírez Ríos et al., 2014). To determine if loss of GAMT affects BCK expression in neurons,

immunostaining analysis of *Gamt*$^{GFP/GFP}$ and control mice at P60 was performed (Fig. **5d**). We found a significant decrease of BCK expression in NeuN^{+} neurons in the motor cortex of *Gamt*$^{GFP/GFP}$ mice compared to control (Fig. **5e**). However, no difference in overall number of neurons in the cortex was observed (Fig. **5f**). Since BCK has been shown to be localized mainly in inhibitory neurons, we also assessed whether the loss of cerebral creatine affected GAD67^{+} inhibitory neuron numbers in mice. Immunostaining analysis revealed *Gamt* deletion had no effect on the total number of inhibitory neurons between (Fig. **5g**). These results suggest that the cerebral creatine deficiency resulted in long term changes in cellular metabolism and bioenergetics, which may lead to neuronal dysregulation without affecting neuronal survival in the adult CNS. Indeed, MRS analysis of *Gamt* knockout mice exhibited increased glutamate/glutamine ratio compared to WT at P56, suggesting altered glutamatergic neurotransmission in the adult CNS (Fig. **5h**).

Inducible knockout of *Gamt* in oligodendrocyte lineage cells leads to reduced oligodendrocytes and inefficient remyelination after demyelinating injury.

We next investigated if *Gamt* expression in oligodendrocytes is required for remyelination. To this end, we crossed our *Gamt*$^{fl/fl}$ line with the *PDGFRα-Cre*^{ERT} mouse line, and generated *PDGFRα-Cre*^{ERT};*Gamt*$^{fl/fl}$ to allow tamoxifen inducible knockout (iKO) of *Gamt* in oligodendrocyte lineage cells (Fig. **6a**). To induce *Gamt* deletion in oligodendrocyte lineage cells, tamoxifen was injected intraperitoneally into mice at 10-11 weeks of age for four consecutive days, and focal experimental demyelination was then performed by lysolecithin injection into the mouse spinal cord ventral white matter.

Sibling tamoxifen-injected *Gamt*$^{fl/fl}$ mice without *PDGFRα-Cre*^{ERT} expression were used as controls. To confirm *Gamt* deletion, we examined the expression of GFP in the lesioned spinal cord of *PDGFRα-Cre*^{ERT};*Gamt*$^{fl/fl}$ iKO and control mice. At 5 days post lesion (dpl), when OPCs are expected to migrate and proliferate into lesions, we did not observe any GFP expression in or outside of the lesions of *PDGFRα-Cre*^{ERT};*Gamt*$^{fl/fl}$ iKO or control mice (Fig. **6b**), suggesting that *Gamt* is not expressed at the OPC recruitment stage during remyelination. The lack of GFP expression also suggested that no mature oligodendrocytes that survived the lesion expressed GFP. However, at 10 dpl, when OPC are expected to have differentiated into oligodendrocytes, we found that GFP was expressed only in CC1$^+$ oligodendrocytes in lesions and barely detectable outside of lesions (Fig. **6c**). Quantification of GFP labeled oligodendrocytes showed approximately 79% of mature oligodendrocytes expressed GFP in lesions (Fig. **6d**), suggesting that GFP$^+$ oligodendrocytes were derived from OPCs that migrated into the lesion during remyelination. These results demonstrate the inducible GFP tagging approach using the *PDGFRα-Cre*^{ERT};*Gamt*$^{fl/fl}$ line allows for the tracking of newly regenerated oligodendrocytes in lesions, and the identification of *Gamt* deleted oligodendrocytes after demyelinating injury.

To determine if tamoxifen induced *Gamt* deletion in oligodendrocyte lineage cells affected oligodendrocyte lineage cell progression in lesions, immunostaining analysis for oligodendrocyte lineage cell markers was performed. We detected a significant reduction of Olig2$^+$ oligodendrocyte lineage cells and CC1$^+$ oligodendrocytes in lesions in the *PDGFRα-Cre*^{ERT};*Gamt*$^{fl/fl}$ iKO compared to control at 10 dpl (Fig. **6e–g**).

Moreover, MBP coverage in the lesion, which is an indicator of remyelination, was significantly reduced at 20 dpl (Fig. **6h** and **i**). These results suggest that creatine synthesis in oligodendrocytes is necessary for efficient oligodendrocyte maturation and remyelination.

Creatine or cyclocreatine supplemented recovery diet leads to increased mature oligodendrocytes and enhanced remyelination after cuprizone-mediated demyelination.

Since 50% of creatine in human comes from diet, we next asked if dietary creatine is important in regulating the function of oligodendrocyte lineage cells with intact *Gamt* expression under demyelinating environment. To this end, wild type mice were fed a 0.2 percent cuprizone in either creatine deficient or standard rodent diet for five weeks, starting at eight weeks-old. (Fig. **7a**). We found that mice on the creatine deficient diet displayed a significant reduction in $Olig2^+$ oligodendrocyte lineage cells and $CC1^+$ oligodendrocytes in the corpus callosum after five weeks of cuprizone treatment compared to those on regular rodent diet (Fig. **7b–d**). Moreover, we observed a significant reduction in $NKX2.2^+$ OPCs (Fig. **7e** and **f**). These data suggest that the absence of dietary creatine leads to a greater loss of the entire oligodendrocyte lineage during cuprizone intoxication, suggesting dietary creatine is protective against oligodendrocyte lineage cell loss and may be necessary to rapidly replenish cerebral creatine pools to lessen the effects of systemic cuprizone toxicity.

To determine if introduction of creatine into rodent diet enhances remyelination, a diet without cuprizone and containing 2% creatine or 0.1% cyclocreatine, a planar creatine analog with greater brain penetrance, were fed to mice for 2 weeks during the recovery period (Fig **7a**) after 5 weeks of cuprizone demyelination. Control mice were fed a creatine deficient diet throughout the experiment. We found that both creatine and cyclocreatine fed mice displayed increased $Olig2^{+}CC1^{+}$ oligodendrocytes (Fig. **8a** and **b**), and significantly greater Fluoromyelin staining (Fig. **8c** and **d**) in the corpus callosum compared to control after two weeks of being on the recovery diet. Electron microscopy analysis revealed that creatine and cyclocreatine diets led to more remyelinated axons compared to control, and displayed lower g-ratios (Fig. **8e and f, g**). These results suggest that dietary creatine significantly enhances CNS remyelination.

DISCUSSION

Creatine synthesis through *Gamt* supports oligodendrocyte maturation and survival during developmental myelination.

Studying CCDS using cellular specific removal of *Gamt* could aid in understanding the etiology behind the development of the intellectual disabilities, seizures and behavior disorders in these patients. These clinical symptoms in patients suggest that the CNS is particularly vulnerable to creatine deficiency (Giusti et al., 2019). We have performed magnetic resonance spectroscopy analysis and showed that cerebral creatine levels are dependent on *Gamt* expression. Moreover, we have now generated a new transgenic mouse model to allow GFP tagging of cells normally displaying creatine synthesis and to determine the effect of endogenous creatine loss on cellular function. Due to large

energy demands required for developmental myelination, we hypothesized that endogenous creatine synthesis may support this process. We found that *Gamt* is not expressed in OPCs, but is expressed in a small portion of premyelinating oligodendrocytes and highly expressed in mature oligodendrocytes, suggesting that creatine is necessary for oligodendrocyte maturation and myelination. Our $Gamt^{GFP/GFP}$ knockout model showed significant reductions in mature oligodendrocytes and myelin proteins at P14 and P21 which coincides with increased cell death in premyelinating oligodendrocytes. These data suggest that endogenously synthesized creatine may support the survival of premyelinating oligodendrocytes and their transition to mature myelinating oligodendrocytes (Hughes and Stockton, 2021). However, the reduction of oligodendrocytes was no longer observed in $Gamt^{GFP/GFP}$ mice compared to controls by P60, suggesting that endogenous creatine synthesis is not required for myelination in mice, but may be necessary to ensure that oligodendrocyte maturation and myelination occur in a timely manner in the postnatal brain. It is known that alterations in the CNS critical windows of development can have long lasting impacts on brain function (Marín, 2016). Importantly, the lack of any overt behavioral perturbations in our mouse model highlights the important difference in neocortical development and white matter volume between humans and rodents.

We also found widespread activation of AMPK signaling in mice lacking *Gamt* expression. Short term activation of AMPK has been shown to protect oligodendrocytes and neurons from cell death, however, long term activation under creatine deficiency may cause a metabolic shift in the CNS leading to prolonged activation of catabolic

pathways (Paintlia et al., 2013; Hardie et al., 2012). Moreover, we found a shift in neuronal bioenergetics in mice lacking *Gamt* expression, in which neurons in the adult CNS exhibited decreased expression of brain creatine kinase at P60. It remains to be determined whether the dysregulation in neuronal bioenergetics is due to: a) a reduced supply of creatine from oligodendrocytes, b) a decreased number of oligodendrocytes during development, c) less metabolically healthy oligodendrocytes, or d) an unknown role of *Gamt* expression in neural stem cell differentiation or function early in development. Although we showed that *Gamt* is uniquely expressed in mature oligodendrocytes starting at P14, it also remained to be confirmed whether oligodendrocyte-derived creatine can be distributed to other cell types in the brain.

Creatine synthesis through GAMT and dietary creatine supplementation support remyelination.

We found that oligodendrocytes synthesized creatine is important for the process of remyelination when lysolecithin induced demyelination was performed on tamoxifen injected *PDGFRα-Cre*^{ERT};*Gamt*$^{fl/fl}$ iKO mice. This result supports our previous work and confirms that no other cell types express *Gamt* under injury (Chamberlain et al., 2017). The inducible strategy ensured that any long term effects of the loss of endogenous creatine during development did not influence our results in the remyelination experiments. Interestingly, we saw no expression of the GFP reporter at 5 dpl and only in mature oligodendrocytes in the lesion at 10 dpl, and thus, suggesting that the GFP tagged oligodendrocytes in lesions are newly regenerated oligodendrocytes involved in remyelination. The inducible GFP tagging approach may be useful for the identification

and tracking of newly regenerated oligodendrocytes and could be incorporated into other animal models of demyelination or experimental injury.

Since half of daily creatine level in humans comes from diet, we investigated whether creatine is important during demyelination and remyelination using a toxic demyelination cuprizone method (Torkildsen et al., 2008). Here, we used a wild-type mouse to see if dietary creatine and cyclocreatine, a lipophilic analog with greater brain penetrance, can speed up the rate of remyelination after cuprizone. Interestingly, both creatine and cyclocreatine increased the number of oligodendrocytes and improved remyelination but there was no significant difference between the two diets. Increasing the cyclocreatine dose or limiting the length of recovery diet may allow us to see greater differences between the diets. Overall, this experiment suggests that creatine supplementation can limit the extent of demyelination and improve the rate of remyelination.

In conclusion, our study showed that *Gamt* is uniquely expressed in mature oligodendrocytes during active myelination, suggesting that oligodendrocytes are the main source of creatine synthesis in the adult CNS. Loss of *Gamt* led to impairments in developmental myelination and remyelination after injury, and that dietary creatine can enhance CNS remyelination. Furthermore, the lack of endogenous creatine synthesis may have long term implications for neuronal energetics and metabolism. These results suggest oligodendrocyte dysfunction might contribute to the CNS pathophysiology associated with CCDS, and that therapeutic strategies targeting oligodendrocyte survival or energetics might reduce neurological impairment in CCDS.

REFERENCES

Albanese C, Rodriguez OC, VanMeter J, Fricke ST, Rood BR, Lee Y, Wang SS, Madhavan S, Gusev Y, Petricoin EF, Wang Y (2013) Preclinical magnetic resonance imaging and systems biology in cancer research: current applications and challenges. Am J Pathol 182:312–318.

Baker SA, Gajera CR, Wawro AM, Corces MR, Montine TJ (2021) GATM and GAMT synthesize creatine locally throughout the mammalian body and within oligodendrocytes of the brain. Brain Research 1770:147627.

Braissant O, Henry H, Béard E, Uldry J (2011) Creatine deficiency syndromes and the importance of creatine synthesis in the brain. Amino Acids 40:1315–1324.

Braissant O, Henry H, Villard A-M, Speer O, Wallimann T, Bachmann C (2005) Creatine synthesis and transport during rat embryogenesis: spatiotemporal expression of AGAT, GAMT and CT1. BMC Dev Biol 5:9.

Chamberlain KA, Chapey KS, Nanescu SE, Huang JK (2017) Creatine Enhances Mitochondrial-Mediated Oligodendrocyte Survival After Demyelinating Injury. J Neurosci 37:1479–1492.

Dimas P, Montani L, Pereira JA, Moreno D, Trötzmüller M, Gerber J, Semenkovich CF, Köfeler HC, Suter U (n.d.) CNS myelination and remyelination depend on fatty acid synthesis by oligodendrocytes. eLife 8:e44702.

Fard MK, van der Meer F, Sánchez P, Cantuti-Castelvetri L, Mandad S, Jäkel S, Fornasiero EF, Schmitt S, Ehrlich M, Starost L, Kuhlmann T, Sergiou C, Schultz V, Wrzos C, Brück W, Urlaub H, Dimou L, Stadelmann C, Simons M (2017) BCAS1 expression defines a population of early myelinating oligodendrocytes in multiple sclerosis lesions. Sci Transl Med 9:eaam7816.

Fricke ST, Rodriguez O, Vanmeter J, Dettin LE, Casimiro M, Chien CD, Newell T, Johnson K, Ileva L, Ojeifo J, Johnson MD, Albanese C (2006) In vivo magnetic resonance volumetric and spectroscopic analysis of mouse prostate cancer models. Prostate 66:708–717.

Fünfschilling U, Supplie LM, Mahad D, Boretius S, Saab AS, Edgar J, Brinkmann BG, Kassmann CM, Tzvetanova ID, Möbius W, Diaz F, Meijer D, Suter U, Hamprecht B, Sereda MW, Moraes CT, Frahm J, Goebbels S, Nave K-A (2012) Glycolytic oligodendrocytes maintain myelin and long-term axonal integrity. Nature 485:517–521.

Giusti L, Molinaro A, Alessandrì MG, Boldrini C, Ciregia F, Lacerenza S, Ronci M, Urbani A, Cioni G, Mazzoni MR, Pizzorusso T, Lucacchini A, Baroncelli L (2019) Brain mitochondrial proteome alteration driven by creatine deficiency suggests

588 novel therapeutic venues for creatine deficiency syndromes. Neuroscience
589 409:276–289.

590 Hardie DG, Ross FA, Hawley SA (2012) AMPK: a nutrient and energy sensor that
591 maintains energy homeostasis. Nat Rev Mol Cell Biol 13:251–262.

592 Harris JJ, Attwell D (2012) The Energetics of CNS White Matter. J Neurosci 32:356–
593 371.

594 Hughes EG, Stockton ME (2021) Premyelinating Oligodendrocytes: Mechanisms
595 Underlying Cell Survival and Integration. Frontiers in Cell and Developmental
596 Biology 9:1985.

597 Lee Y, Morrison BM, Li Y, Lengacher S, Farah MH, Hoffman PN, Liu Y, Tsingalia A, Jin
598 L, Zhang P-W, Pellerin L, Magistretti PJ, Rothstein JD (2012) Oligodendroglia
599 metabolically support axons and contribute to neurodegeneration. Nature
600 487:443–448.

601 Lowe MTJ, Kim EH, Faull RLM, Christie DL, Waldvogel HJ (2013) Dissociated
602 expression of mitochondrial and cytosolic creatine kinases in the human brain: a
603 new perspective on the role of creatine in brain energy metabolism. J Cereb
604 Blood Flow Metab 33:1295–1306.

605 Marín O (2016) Developmental timing and critical windows for the treatment of
606 psychiatric disorders. Nat Med 22:1229–1238.

607 Paintlia AS, Paintlia MK, Mohan S, Singh AK, Singh I (2013) AMP-Activated Protein
608 Kinase Signaling Protects Oligodendrocytes that Restore Central Nervous
609 System Functions in an Experimental Autoimmune Encephalomyelitis Model. Am
610 J Pathol 183:526–541.

611 Ramírez Ríos S, Lamarche F, Cottet-Rousselle C, Klaus A, Tuerk R, Thali R, Auchli Y,
612 Brunisholz R, Neumann D, Barret L, Tokarska-Schlattner M, Schlattner U (2014)
613 Regulation of brain-type creatine kinase by AMP-activated protein kinase:
614 interaction, phosphorylation and ER localization. Biochim Biophys Acta
615 1837:1271–1283.

616 Rinholm JE, Hamilton NB, Kessaris N, Richardson WD, Bergersen LH, Attwell D (2011)
617 Regulation of Oligodendrocyte Development and Myelination by Glucose and
618 Lactate. J Neurosci 31:538–548.

619 Sirajuddin P et al. (2012) Quantifying the CDK inhibitor VMY-1-103's activity and tissue
620 levels in an in vivo tumor model by LC-MS/MS and by MRI. Cell Cycle 11:3801–
621 3809.

622 Sturrock RR (1980) Myelination of the mouse corpus callosum. Neuropathol Appl
623 Neurobiol 6:415–420.

Tachikawa M, Fukaya M, Terasaki T, Ohtsuki S, Watanabe M (2004) Distinct cellular expressions of creatine synthetic enzyme GAMT and creatine kinases uCK-Mi and CK-B suggest a novel neuron-glial relationship for brain energy homeostasis. Eur J Neurosci 20:144–160.

Tachikawa M, Watanabe M, Fukaya M, Sakai K, Terasaki T, Hosoya K-I (2018) Cell-Type-Specific Spatiotemporal Expression of Creatine Biosynthetic Enzyme S-adenosylmethionine:guanidinoacetate N-methyltransferase in Developing Mouse Brain. Neurochem Res 43:500–510.

Torkildsen O, Brunborg LA, Myhr K-M, Bø L (2008) The cuprizone model for demyelination. Acta Neurol Scand Suppl 188:72–76.

Wyss M, Braissant O, Pischel I, Salomons GS, Schulze A, Stockler S, Wallimann T (2007) Creatine and creatine kinase in health and disease--a bright future ahead? Subcell Biochem 46:309–334.

Wyss M, Kaddurah-Daouk R (2000) Creatine and creatinine metabolism. Physiol Rev 80:1107–1213.

Yan H, Rivkees SA (2006) Hypoglycemia influences oligodendrocyte development and myelin formation. Neuroreport 17:55–59.

FIGURE LEGENDS

Fig 1. Endogenously synthesized creatine supplies cerebral creatine and is dependent on *Gamt* expression. a) Diagram of *Gamt* knockout (KO) transgenic mouse model **b)** Region of magnetic resonance spectroscopy (MRS) voxel placement in mouse prefrontal cortex **c)** Representative trace from MRS from each group **d)** Quantification of metabolites, normalized to choline, showing unmeasurable creatine levels in the brain in the KO on creatine deficient diet (one-way ANOVA with Tukey's multiple comparisons; $F(3, 8)=83.81$, $df=11$, $p<0.0001$) and normal levels of creatine in the WT on creatine deficient diet (WT normal vs. WT crt def $p=0.70$, ns). KO on a normal diet had measurable, but significantly reduced levels of creatine compared to WT (KO normal vs. WT normal $p=0.02$). All data presented as mean±SEM with n=3 biological replicates. Data presented with *p<0.05, **p<0.01, ***p<0.001, ****p<0.0001, ns= not significant.

Fig 2. *Gamt* knock-in reporter mouse shows *Gamt* becomes highly expressed and restricted to oligodendrocyte lineage cells during active myelination. a) Diagram of transgenic mouse model showing heterozygous expression of *Gamt* with GFP expression. Postnatal (P) day P7 co-immunostaining analysis of GFP and **b)** $Nestin^+$ cells around the subventricular zone (SVZ), **c)** $Nestin^+$ cells at the adjacent striatum, **d)** $Olig2^+$ oligodendrocyte lineage cells, and **e)** $GFAP^+$ astrocytes in the corpus callosum. SVZ is outlined in white dotted line b-e. P14 co-immunostaining analysis of GFP and **f)** $GFAP^+$ astrocytes, **g)** $Iba1^+$ microglia/macrophages, **h)** $NeuN^+$ neurons, **i)** $Olig2^+$ oligodendrocyte lineage cells, **j)** $NKX2.2^+$ OPCs, **k)** $BCAS1^+$ premyelinating

oligodendrocytes, and **l)** CC1$^+$ oligodendrocytes in the corpus callosum. **m)** Percentage of OPCs, premyelinating and mature oligodendrocytes that express GFP. All data presented as mean±SEM with n=3 biological replicates. Scale bar is 20μm in b,c and 50μm in all other images.

Fig 3. Deletion of *Gamt* results in reduced mature oligodendrocytes at P14 and P21 and a delay in developmental myelination. a) Diagram of *Gamt*$^{GFP/GFP}$ knockout mouse (top) and confirmation of GAMT deletion by western blot (bottom). **b)** Immunostaining of control and *Gamt*$^{GFP/GFP}$ for Olig2$^+$ oligodendrocyte lineage cells and CC1$^+$ oligodendrocytes in the corpus callosum at P14. **c)** Quantification showing total Olig2$^+$ oligodendrocyte lineage cells at P14 (two-way ANOVA of genotype x age with Sidak's multiple comparisons; F (1, 4)=19.77, df=1 for genotype; p=0.01), CC1$^+$ oligodendrocytes in the corpus callosum at P14 and P21 (two-way ANOVA with Sidak's multiple comparisons; F (1, 12)=33.86, df=1, p<0.0001), and **d)** NKX2.2$^+$ OPC numbers (p=0.1, ns). **e)** Myelin basic protein (MBP) staining coverage at P21 is reduced in *Gamt*$^{GFP/GFP}$ compared to controls. **f)** Quantification of MBP coverage at P21 (two-tailed t-test; t=4.721, df=4, p=0.009). **g)** Western blot analysis for myelin oligodendrocyte glycoprotein (MOG) expression in *Gamt*$^{GFP/GFP}$ cerebellar extract at P21. **h)** Quantification of MOG expression in *Gamt*$^{GFP/GFP}$ mice (two-tailed t-test; t=4.494, df=4, p=0.01). All data presented as mean±SEM with n=3 biological replicates. Scale bar is 50μm in b,e. Data presented with *p<0.05, **p<0.01.

Fig 4. Deletion of *Gamt* leads to increased death of premyelinating oligodendrocytes in the corpus callosum. a) Olig2 and TUNEL co-staining analysis in the CNS of control and $Gamt^{GFP/GFP}$ knockout mouse at P14. Corpus callosum is outlined with white dashed lines. Arrows point to TUNEL$^+$ cells at the corpus callosum. **b)** Quantification of TUNEL labeling in the corpus callosum at P14 and P21 (two-way ANOVA with Sidak's multiple comparisons; $F(1, 10)=15.18$, df=1, $p=0.003$). **c)** Quantification of TUNEL labeled oligodendrocyte lineage cells at P21 (two-tailed t-test; $t=7.28$, df=4, $p=0.002$). **d)** BCAS1 and TUNEL co-staining in the CNS of control and $Gamt^{GFP/GFP}$ knockout mouse at P14. Corpus callosum is outlined with white dashed lines. **e)** Insets showing colocalization of TUNEL with BCAS1$^+$ premyelinating oligodendrocytes (arrows) at P14. **f)** Ki67$^+$ analysis of control and $Gamt^{GFP/GFP}$ mice shows no difference in cell proliferation at P14 or P21 (two-way ANOVA with Sidak's multiple comparisons; $F(1, 8)=0.06$, $p=0.8134$, ns). All data presented as mean±SEM with n=3-4 biological replicates. Scale bar is 20μm in a, 50μm in d and 5μm in insets. Data presented with *$p<0.05$, **$p<0.01$, ns=not significant.

Fig 5. Loss of *Gamt* leads to activated AMPK signaling and reduced brain creatine kinase (BCK) in the cortex of adult mice. a) Western blot of cerebellar lysates for AMPK signaling in wildtype and $Gamt^{GFP/GFP}$ knockout mouse at P21. **b)** Quantification of total AMPK (two-tailed t-test; $t=2.884$, df=4, $p=0.045$), and **c)** phosphorylated AMPK (two-tailed t-test; $t=6.084$, df=4, $p=0.0037$). **d)** Immunostaining of BCK and NeuN$^+$ neurons in the motor cortex in controls and $Gamt^{GFP/GFP}$ at P60. Quantification of **e)** BCK expression in neurons (two-tailed t-test; $t=4.912$, df=4, $p=0.008$), and **f)** total

neurons in the motor cortex (p=0.16, ns). **g)** Quantification of GAD67+ inhibitory neurons in the motor cortex at P60 (p=0.695, ns). **h)** MRS analysis glutamate-glutamine ratio in GAMT KO on a creatine deficient diet compared to WT on creatine deficient diet at P56 (two-tailed t-test; t=3.417, df=4, p=0.027). All data presented as mean±SEM with n=3 biological replicates. Scale bar is 50μm in d. Data presented with *p<0.05, **p<0.01, ns=not significant.

Fig 6. Deletion of *Gamt* from oligodendrocyte lineage cells leads to reduced mature oligodendrocytes and myelin coverage in lesions during remyelination. a) Diagram showing strategy to delete *Gamt* from oligodendrocyte lineage cells in *PDGFRα-CreERT;Gamt$^{fl/fl}$* mice by i.p. injections of tamoxifen for four days, followed by lysolecithin spinal cord demyelination. **b)** No GFP expression was detected at 5 days post lesion (dpl). **c)** GFP expression in CC1^{+} mature oligodendrocytes in lesions at 10 dpl. **d)** Quantification shows GFP colocalization in 79 percent of mature oligodendrocytes in the lesions. **e)** Immunostaining of Olig2^{+} oligodendrocyte lineage cells in lesion of tamoxifen treated control and *PDGFRα-CreERT;Gamt$^{fl/fl}$* mice. **f)** Quantification showing Olig2^{+} oligodendrocyte lineage cells (two-way ANOVA with Tukey's multiple comparisons; F(1, 8)=13.76, df=1, p=0.006) and **g)** CC1^{+} oligodendrocytes (two-way ANOVA with Tukey's multiple comparisons; F(1, 8)=0.0016, df=1, p=0.0016) in lesions of *PDGFRα-CreERT;Gamt$^{fl/fl}$* iKO compared to control at 10 dpl. **h)** Immunostaining of myelin basic protein (MBP) at 20 dpl. **i)** Quantification showing (MBP) coverage in lesions of *PDGFRα-CreERT;Gamt$^{fl/fl}$* iKO compared to control at 20 dpl (two-tailed t-test; t=3.449, df=4, p=0.026). All data presented as

mean±SEM with n=3 biological replicates. Scale bar is 50μm in b,c,e,h. Data presented with *p<0.05, **p<0.01.

Fig 7. Cuprizone demyelination under creatine deficient diet results in greater loss of oligodendrocytes and oligodendrocyte precursor cells (OPC) in the corpus callosum. a) Diagram of cuprizone experiment and groups. **b)** Images of $Olig2^+CC1^+$ mature oligodendrocytes in the corpus callosum after five weeks of cuprizone with creatine deficient diet compared to cuprizone with normal diet. **c)** Quantification showing $Olig2^+$ oligodendrocyte lineage cells (two-tailed t-test, t=7.717, df=6, p=0.0002) and **d)** $CC1^+$ oligodendrocytes (two-tailed t-test; t=11.38, df=6, p<0.0001) in the corpus callosum. **e)** Images of $Olig2^+NKX2.2^+$ OPCs in corpus callosum after five weeks of cuprizone with creatine deficient diet compared to cuprizone with normal diet. **f)** Quantification showing $NKX2.2^+$ OPCs in the corpus callosum (two-tailed t-test; t=3.819, df=6, p=0.009). All data presented as mean±SEM with n=4 biological replicates. Scale bar is 50μm in b,e. Data presented with *p<0.05, **p<0.01, ***p<0.001, ****p<0.0001.

Fig 8. Creatine or cyclocreatine supplemented recovery diet increases mature oligodendrocytes and enhances remyelination. a) Images of $Olig2^+CC1^+$ mature oligodendrocytes in corpus callosum after two weeks of recovery diet containing either no creatine (Crt Def), 2% creatine, or 0.1% cyclocreatine. **b)** Quantification of $CC1^+$ oligodendrocytes following two weeks of recovery diet (one-way ANOVA with Sidak's multiple comparisons; F(3, 10)=29.58, df=13, p<0.0001). **c)** Images of Fluoromyelin in

corpus callosum after the different recovery diets. **d)** Quantification of Fluoromyelin intensity in the corpus callosum following two weeks of recovery diet (one-way ANOVA with Dunnett's multiple comparisons; $F(3, 11)=4.279$, df=14, $p=0.03$). **e)** EM images of axons in cross sections of corpus callosum from mice under the different recovery diets. Magnification x 5,000. **f** and **g)** G-ratio analysis of myelinated axons in the corpus callosum under the different recovery diets (one-way ANOVA with Tukey's multiple comparisons; $F(2, 237)=40.28$, df=239, $p<0.0001$). All data presented as mean±SEM with n=3-4 biological replicates in a-d. Representative EM analysis in e-g from n=1, 80 axons per animal. Scale bar is 100μm in a,c and 500nm in e. Data presented with *p<0.05, **p<0.01, ***p<0.001, ****p<0.0001, ns= not significant.

Extended Data Fig 2-1. Overview of targeting strategy to generate a *Gamt* GFP knock-in transgenic mouse line. A linearized vector was generated to the *Gamt* gene in C57BL/6 mice on chromosome ten and delivered to embryonic stem cells via electroporation. The targeted allele has loxP sites (purple) flanking exons 2-6 of the *Gamt* gene (yellow). The green Rox site prevents expression of enhanced GFP cassette but upon cre recombination, *Gamt* along with the Rox site are removed and GFP is expressed.

Extended Data Fig 4-1. Removal of *Gamt* leads to reduced fatty acid synthase in the corpus callosum. a) Images of $FASN^{+}CC1^{+}$ cells in the corpus callosum at P21. **b)** Quantification of $FASN^{+}CC1^{+}$ cells (two-tailed t-test; $t=5.88$, df=4, $p=0.0042$). All data

780 presented as mean±SEM with n=3 biological replicates. Scare bar is 50μm in a. Data
781 presented with **p<0.01.

a

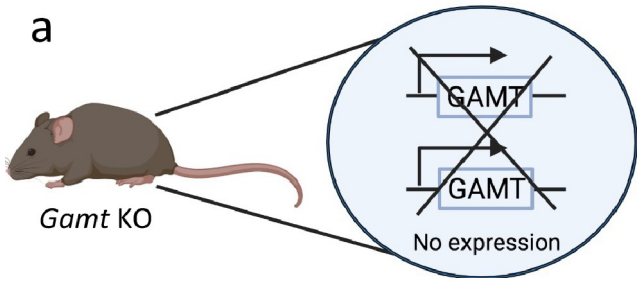
GAMT
GAMT
Gamt KO
No expression

b

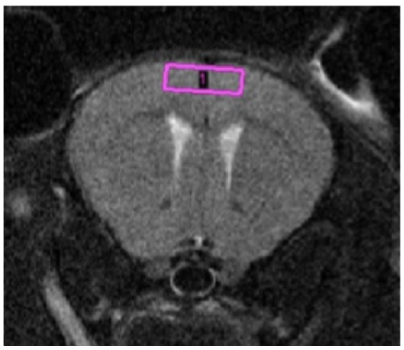

c

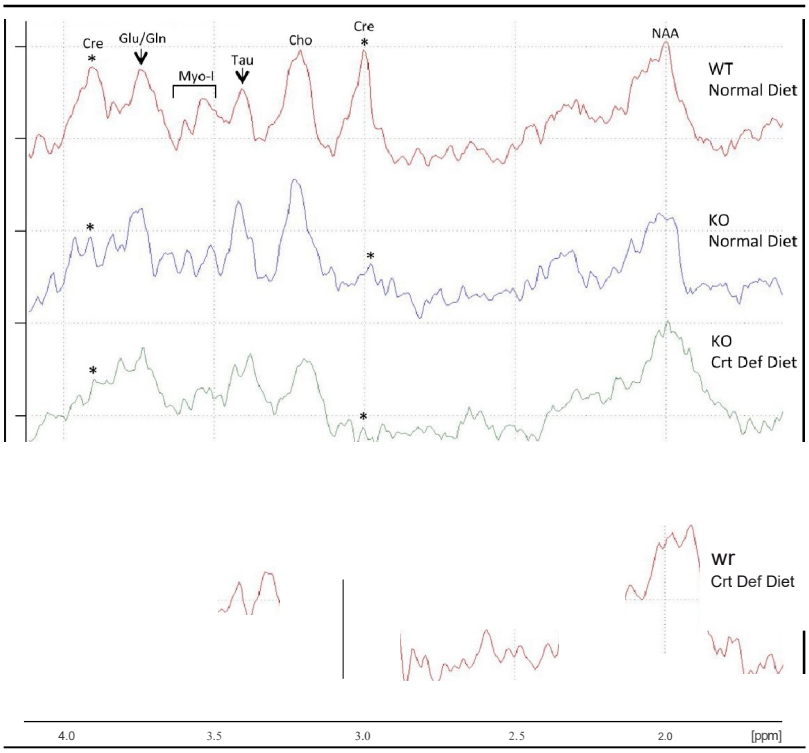
Cre
Glu/Gln
Myo-I
Tau
Cho
Cre
NAA
WT
Normal Diet
KO
Normal Diet
KO
Crt Def Diet
wr
Crt Def Diet
4.0
3.5
3.0
2.5
2.0
[ppm]

d

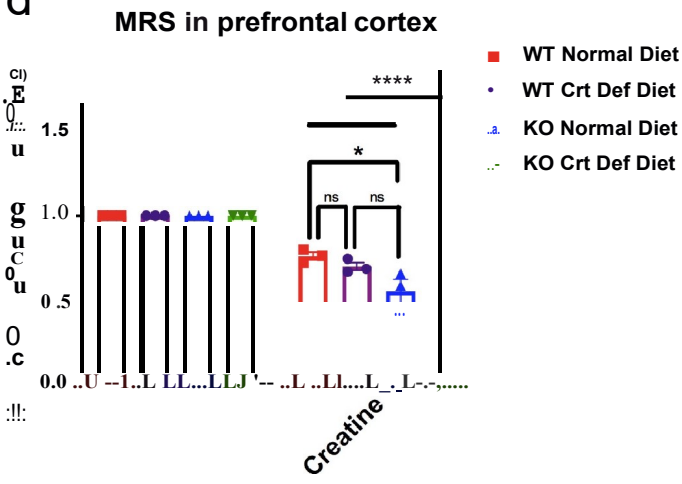
MRS in prefrontal cortex
WT Normal Diet
WT Crt Def Diet
KO Normal Diet
KO Crt Def Diet
1.5
1.0
0.5
0.0
****
*
ns
ns
Creatine

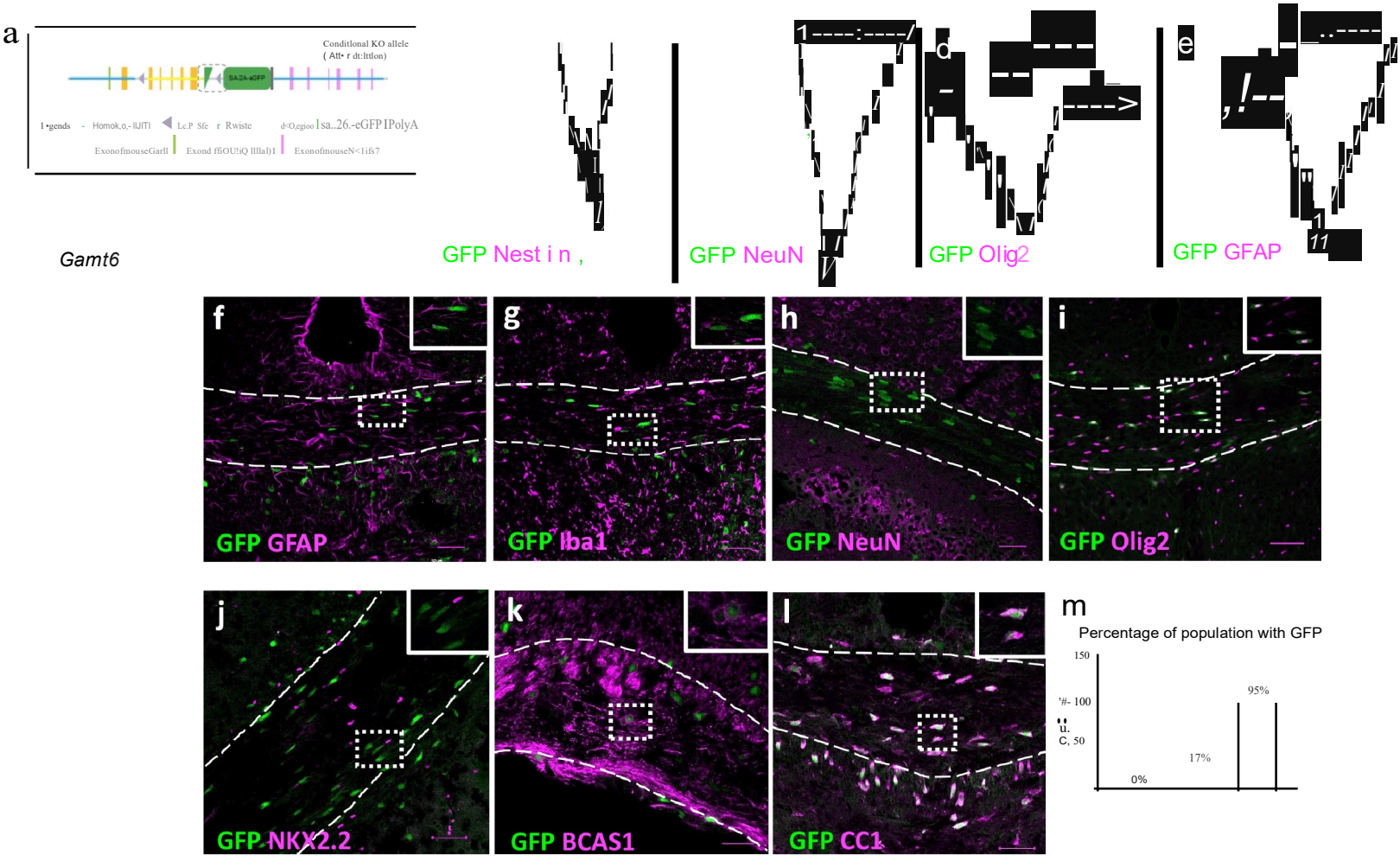
a
Conditional KO allele
(Att• r dt:Ittlon)
SA:2A eGFP
Gamt6
GFP Nest i n ,
GFP NeuN
GFP Olig2
GFP GFAP
f
GFP GFAP
g
GFP Iba1
h
GFP NeuN
i
GFP Olig2
j
GFP NKX2.2
k
GFP BCAS1
l
GFP CC1
m
Percentage of population with GFP
150
100
50
0%
17%
95%

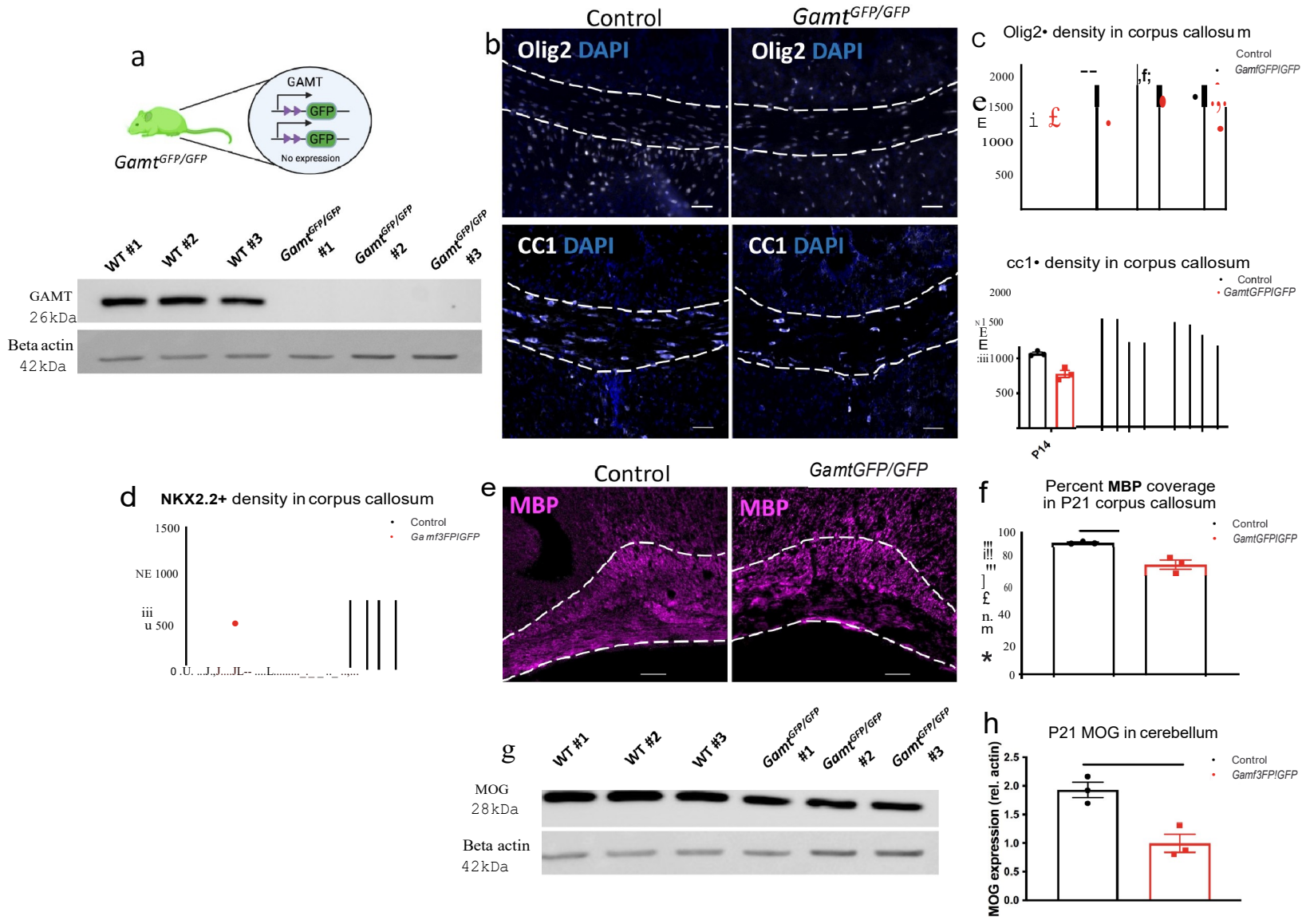
a
GAMT
GFP
GFP
No expression
Gamt GFP/GFP
WT #1
WT #2
WT #3
Gamt GFP/GFP #1
Gamt GFP/GFP #2
Gamt GFP/GFP #3
GAMT
26kDa
Beta actin
42kDa
b
Control
Gamt GFP/GFP
Olig2 DAPI
Olig2 DAPI
CC1 DAPI
CC1 DAPI
c
Olig2• density in corpus callosum
Control
GamfGFP/GFP
2000
1500
1000
500
cc1• density in corpus callosum
Control
GamtGFP/GFP
2000
1500
1000
500
P14
d
NKX2.2+ density in corpus callosum
Control
Gamf3FP/GFP
1500
1000
500
0
e
Control
GamtGFP/GFP
MBP
MBP
f
Percent MBP coverage in P21 corpus callosum
Control
GamtGFP/GFP
100
80
60
40
20
0
g
WT #1
WT #2
WT #3
Gamt GFP/GFP #1
Gamt GFP/GFP #2
Gamt GFP/GFP #3
MOG
28kDa
Beta actin
42kDa
h
P21 MOG in cerebellum
Control
Gamf3FP/GFP
MOG expression (rel. actin)
2.5
2.0
1.5
1.0
0.5
0.0

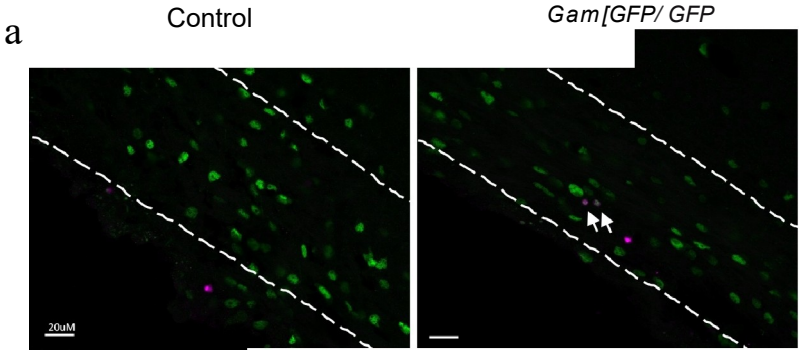
a
Control
Gam[GFP/ GFP
20uM

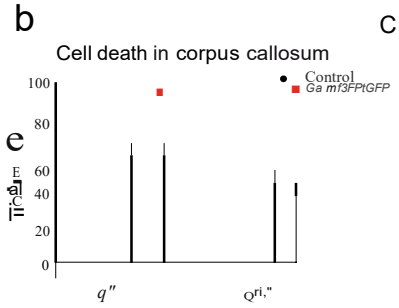
b
Cell death in corpus callosum
Control
Ga mf3FPtGFP
100
80
60
40
20
0

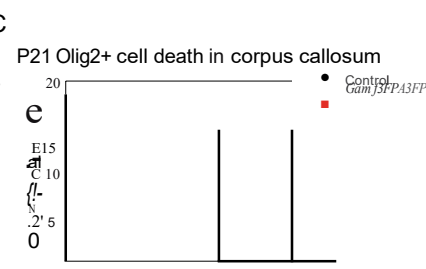
c
P21 Olig2+ cell death in corpus callosum
Control
20
10
5
0

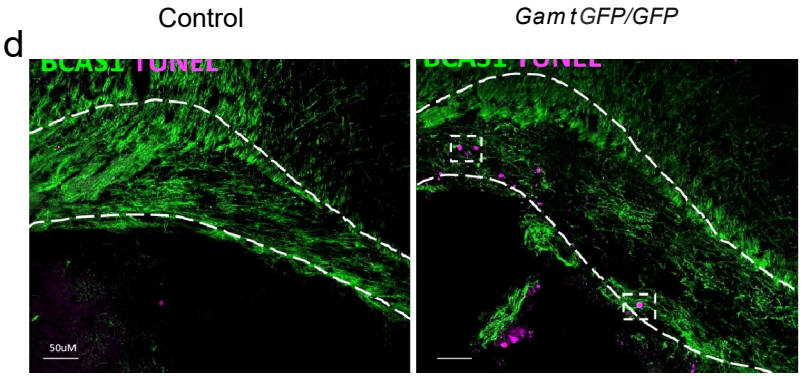
d
Control
GamtGFP/GFP
50uM

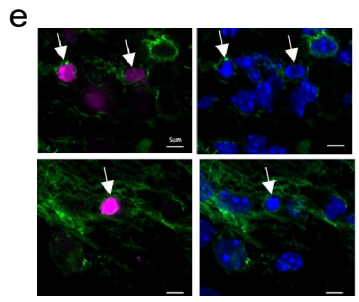
e

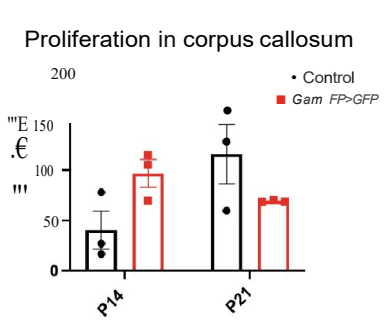
f
Proliferation in corpus callosum
200
150
100
50
0
• Control
Gam FP>GFP
P14
P21

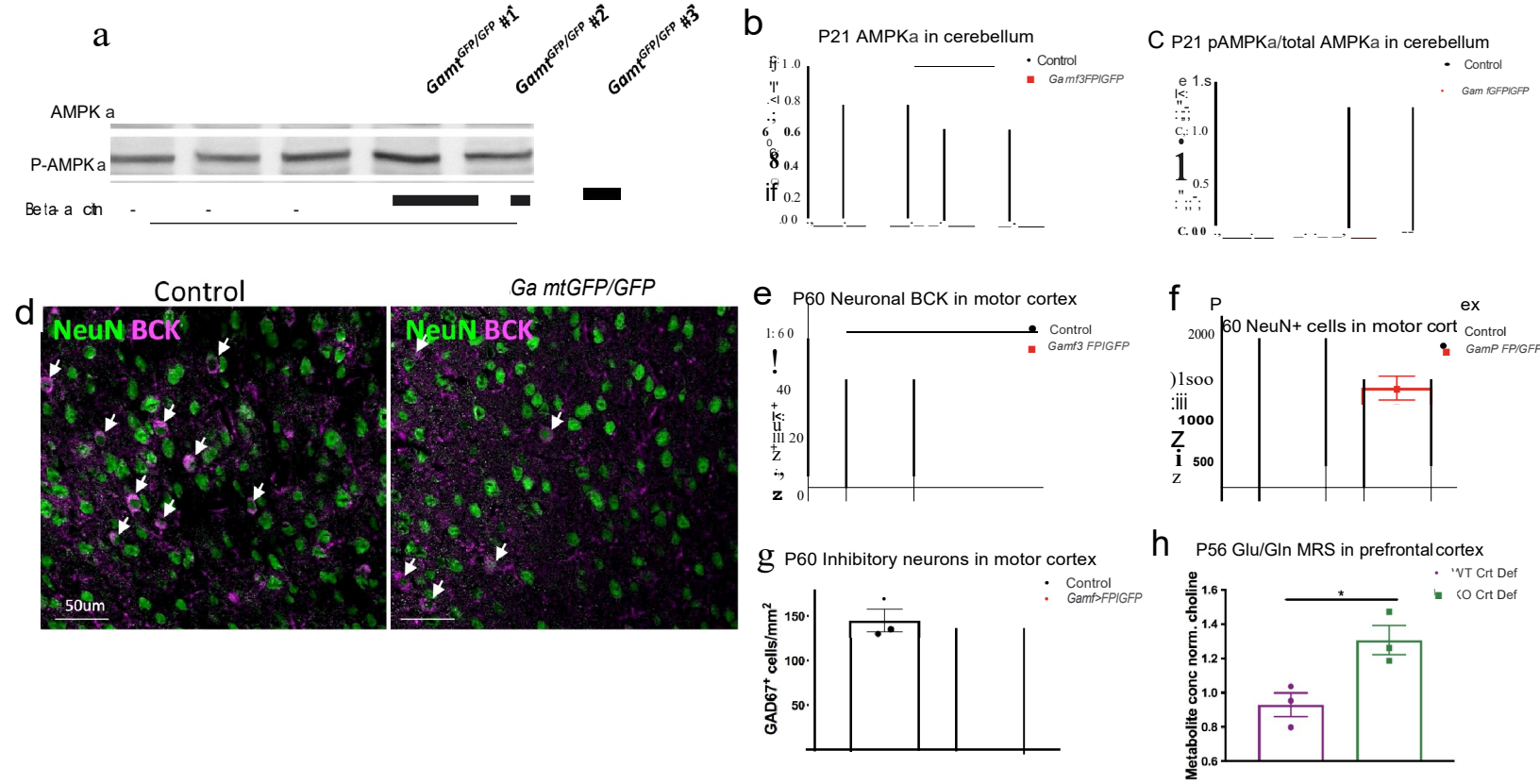
a
Gamt GFP/GFP #1
Gamt GFP/GFP #2
Gamt GFP/GFP #3
AMPK a
P-AMPK a
Beta-a ctin
b
P21 AMPKa in cerebellum
Control
Gamf3FPIGFP
C P21 pAMPKa/total AMPKa in cerebellum
Control
Gam fGFPIGFP
d
Control
Ga mtGFP/GFP
NeuN BCK
NeuN BCK
50um
e
P60 Neuronal BCK in motor cortex
Control
Gamf3 FPIGFP
f
P
ex
60 NeuN+ cells in motor cort
Control
GamP FP/GFP
g
P60 Inhibitory neurons in motor cortex
Control
Gamf>FPIGFP
GAD67+ cells/mm2
h
P56 Glu/Gln MRS in prefrontal cortex
Metabolite conc norm. choline

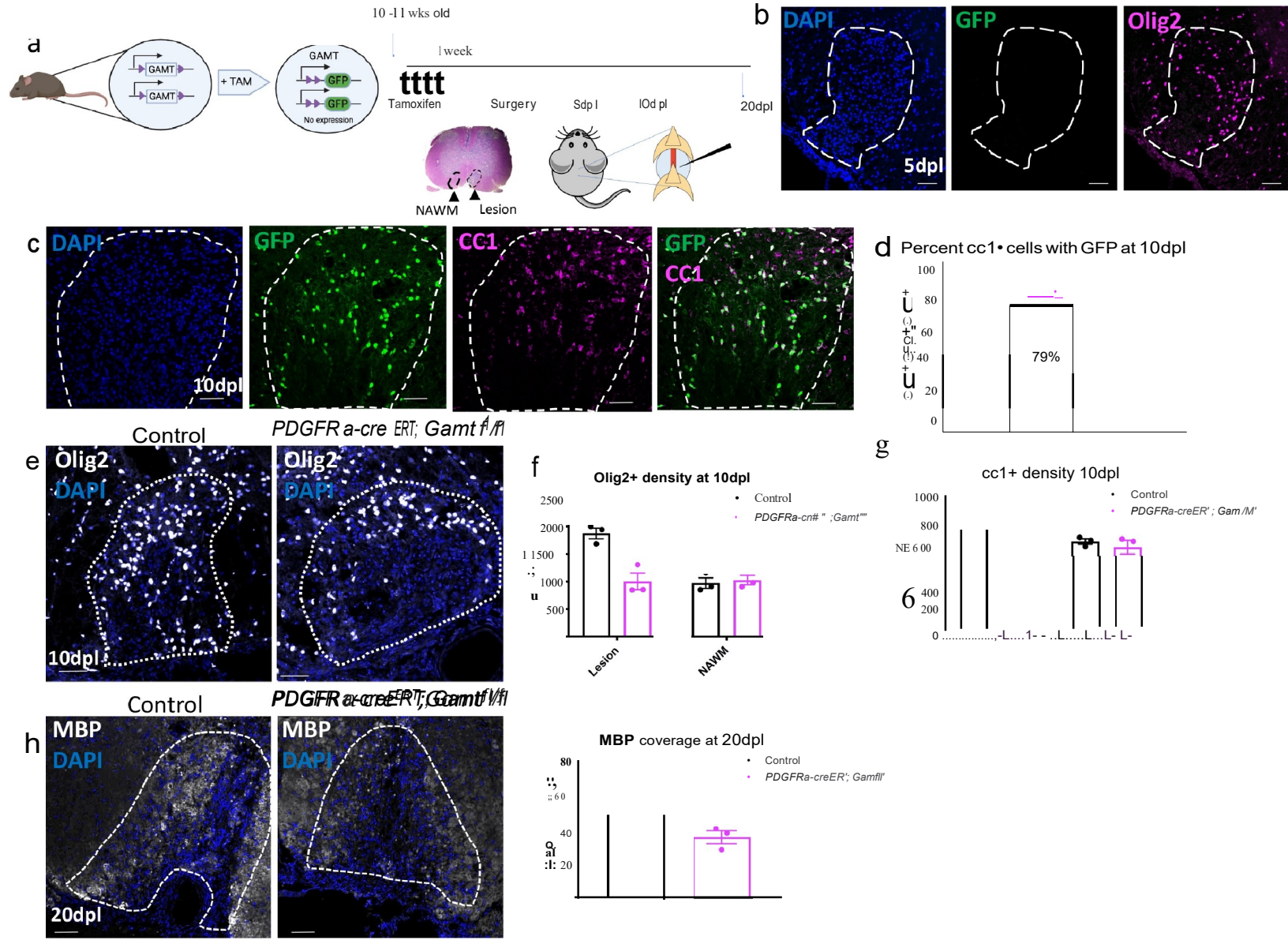
a
10 -l l wks old
GAMT
GAMT
+ TAM
GAMT
GFP
GFP
No expression
l week
tttt
Tamoxifen
Surgery
Sdp l
lOd pl
20dpl
NAWM
Lesion
b
DAPI
GFP
Olig2
5dpl
c
DAPI
GFP
CC1
GFP
CC1
10dpl
d
Percent cc1• cells with GFP at 10dpl
100
80
60
40
20
0
79%
Control
PDGFR a-cre ERT; Gamt f/f
e
Olig2
DAPI
Olig2
DAPI
10dpl
f
Olig2+ density at 10dpl
Control
PDGFRa-cn# " ;Gamt""
2500
2000
1500
1000
500
Lesion
NAWM
g
cc1+ density 10dpl
Control
PDGFRa-creER' ; Gam /M'
1000
800
400
200
0
Control
PDGFR a-creER ; Gamt f/f
h
MBP
DAPI
MBP
DAPI
20dpl
MBP coverage at 20dpl
Control
PDGFRa-creER'; Gamfll'
80
60
40
20

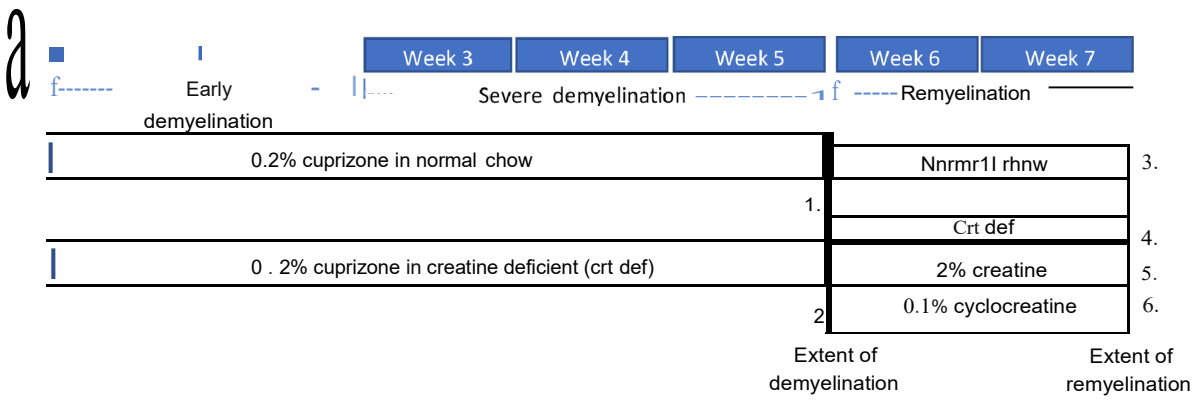
a
Week 3
Week 4
Week 5
Week 6
Week 7
Early demyelination
Severe demyelination
Remyelination
0.2% cuprizone in normal chow
0 . 2% cuprizone in creatine deficient (crt def)
Nnrmr1l rhnw
Crt def
2% creatine
0.1% cyclocreatine
1.
2
3.
4.
5.
6.
Extent of demyelination
Extent of remyelination

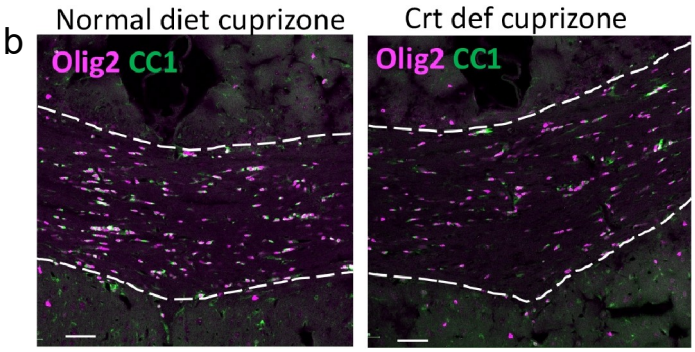
b
Normal diet cuprizone
Crt def cuprizone
Olig2 CC1
Olig2 CC1

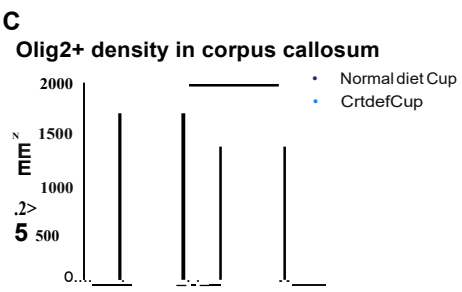
c
Olig2+ density in corpus callosum
Normal diet Cup
CrtdefCup
2000
1500
1000
500
0

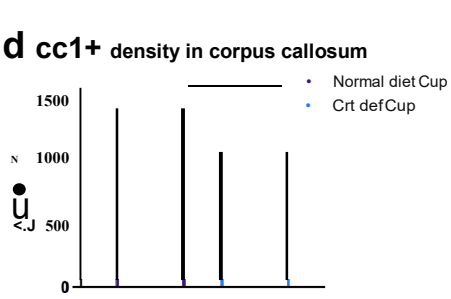
d cc1+ density in corpus callosum
Normal diet Cup
Crt def Cup
1500
1000
500
0

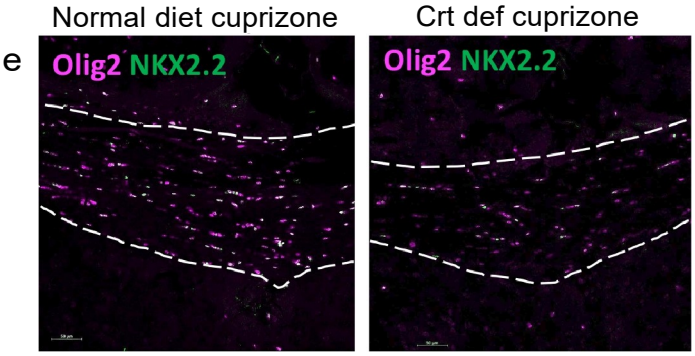
e
Normal diet cuprizone
Crt def cuprizone
Olig2 NKX2.2
Olig2 NKX2.2

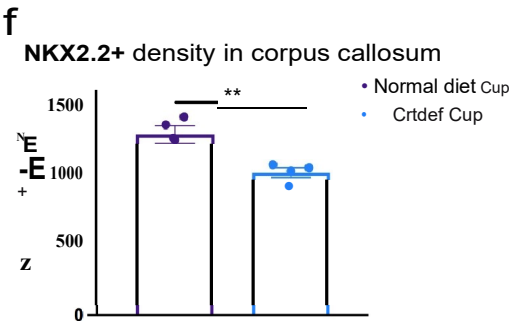
f
NKX2.2+ density in corpus callosum
Normal diet Cup
Crtdef Cup
**
1500
1000
500
0

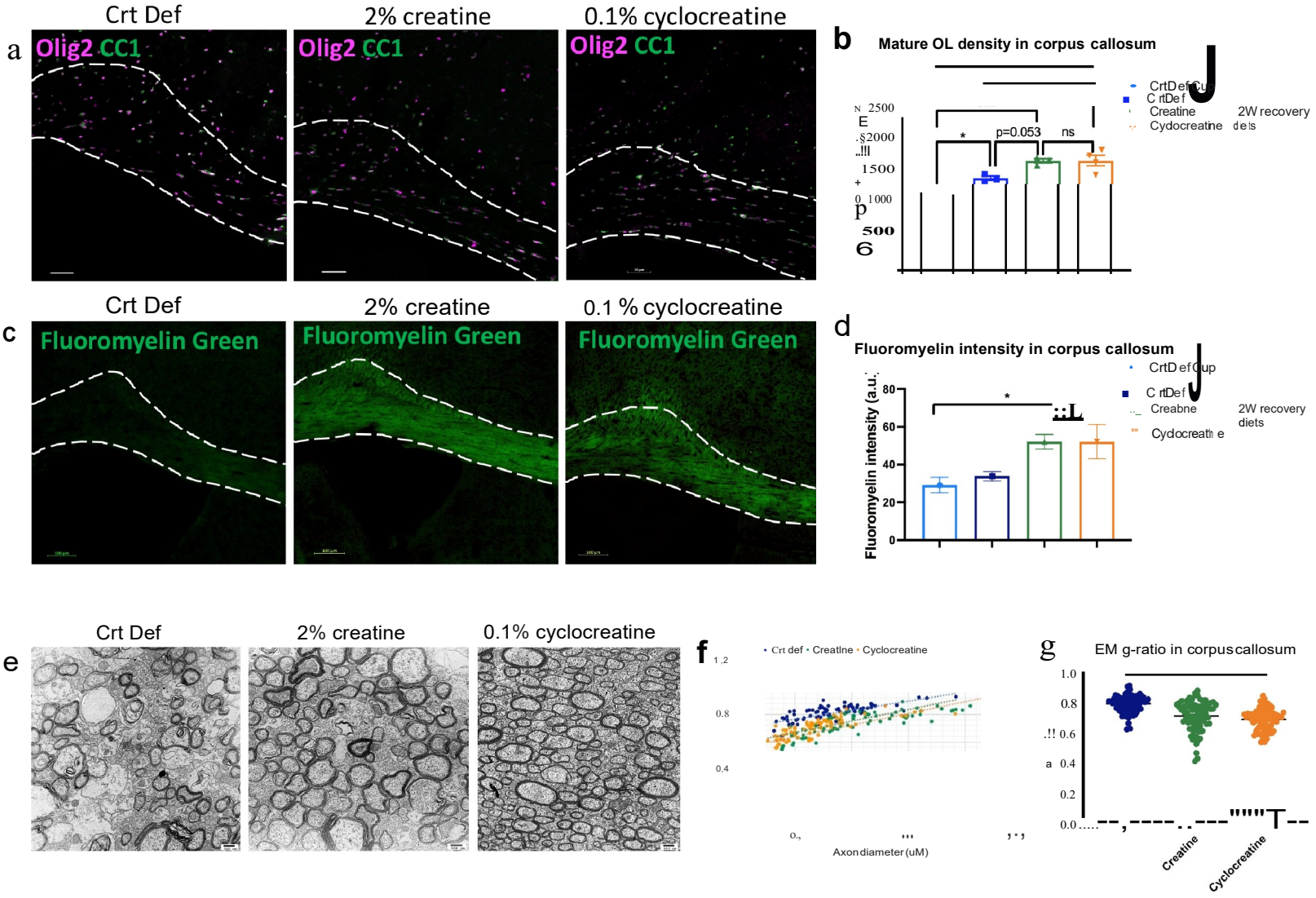
Crt Def
2% creatine
0.1% cyclocreatine
a
Olig2 CC1
Olig2 CC1
Olig2 CC1
b
Mature OL density in corpus callosum
p=0.053
ns
Creatine
Cydocreatine
2W recovery
diets
Crt Def
2% creatine
0.1 % cyclocreatine
c
Fluoromyelin Green
Fluoromyelin Green
Fluoromyelin Green
d
Fluoromyelin intensity in corpus callosum
Fluoromyelin intensity (a.u.)
Creabne
Cydocreath e
2W recovery
diets
Crt Def
2% creatine
0.1% cyclocreatine
e
f
Crt def
Creatine
Cyclocreatine
Axon diameter (uM)
g
EM g-ratio in corpus callosum
Creatine
Cyclocreatine